

AN ANALYSIS OF THE GENERAL INSTABILITY OF ECCENTRICALLY
STIFFENED COMPLETE SPHERICAL SHELLS UNDER UNIFORM PRESSURE

A THESIS

Presented to
The Faculty of the Graduate Division

by
Robert T. Cole

In Partial Fulfillment
of the Requirements for the Degree
Doctor of Philosophy
in the School of Aerospace Engineering

Georgia Institute of Technology

July, 1969

In presenting the dissertation as a partial fulfillment of the requirements for an advanced degree from the Georgia Institute of Technology, I agree that the Library of the Institute shall make it available for inspection and circulation in accordance with its regulations governing materials of this type. I agree that permission to copy from, or to publish from, this dissertation may be granted by the professor under whose direction it was written, or, in his absence, by the Dean of the Graduate Division when such copying or publication is solely for scholarly purposes and does not involve potential financial gain. It is understood that any copying from, or publication of, this dissertation which involves potential financial gain will not be allowed without written permission.

7/25/68

AN ANALYSIS OF THE GENERAL INSTABILITY OF ECCENTRICALLY
STIFFENED COMPLETE SPHERICAL SHELLS UNDER UNIFORM PRESSURE

Approved:

Chairman

Date approved by Chairman:

8/25/69

ACKNOWLEDGMENTS

I wish to express my deepest appreciation to Dr. George J. Simitses who suggested this thesis topic and provided the encouragement and guidance necessary for the completion of this research. To Drs. Lawrence W. Rehfield, C. V. Smith, and Marvin B. Sledd I owe special thanks for their many hours of fruitful discussion during the investigation and the preparation of the manuscript. I also thank Dr. James C. Wang for his patient examination of the manuscript.

I owe a special debt of gratitude to Dr. James A. Stricklin who provided encouragement in my early years of graduate work, to Dr. S. P. Chan who supplied many helpful references, to James H. Sams who was instrumental in the attainment of summer jobs, and to my parents, Mr. and Mrs. Joseph T. Cole, for their neverending kindness and understanding.

The financial assistance of the National Defense Education Act and the Georgia Institute of Technology are gratefully acknowledged.

To Mrs. Betty R. Sims I express my thanks for her patience and skill in typing the final draft of this thesis.

My wife, Sally, has provided continual love, understanding, and encouragement. Without her this work would never have been started, much less finished.

TABLE OF CONTENTS

	Page
ACKNOWLEDGMENTS	ii
LIST OF TABLES	v
LIST OF ILLUSTRATIONS	vi
NOMENCLATURE	vii
SUMMARY	xi
Chapter	
I. GENERAL INTRODUCTION	1
Historical Background	
Scope of the Analysis	
II. LINEAR ANALYSIS	9
Introductory Remarks	
Formulation of the Problem	
Buckling Analysis	
Weight Savings	
Discussion and Conclusions	
III. AXISYMMETRIC INITIAL POST-BUCKLING ANALYSIS	29
Introductory Remarks	
The Energy Functional	
Strain Energy of the Shell	
Potential Energy of the Load	
The First Expansion of the Energy Functional	
Primary State	
The Second Expansion of the Energy Functional	
Eigenvalue Analysis	
Stability Equations	
Reduction of the Equations	
Solution of the Stability Equations	
Imperfection-Sensitivity Study	
General Procedure	
Evaluation of the Required Functionals	
Completion of the Study	
Discussion and Conclusions	

Chapter	Page
APPENDIX	
A. DERIVATION OF THE CRITICAL CONDITION.	68
B. THE TWO PROGRAMS FROM THE LINEAR ANALYSIS	73
Making the Mushtari-Vlasov-Donnell Approximation	
Not Making the Mushtari-Vlasov-Donnell Approximation	
C. REDUCTION OF THE ENERGY FUNCTIONALS	77
D. THE PROGRAM FOR THE IMPERFECTION-SENSITIVITY STUDY.	81
BIBLIOGRAPHY	83
VITA	89

LIST OF TABLES

Table		Page
1.	Sample Results from Both Programs from the Linear Analysis.	52
2.	Initial Post-Buckling Slopes Suggested by the Koiter Analysis.	53

LIST OF ILLUSTRATIONS

Figure		Page
1.	Geometry and Sign Convention.	54
2.	The Effect of Stiffener Eccentricity.	55
3.	The Effect of ρ on the General Instability Loads.	58
4.	The Effect of ρ on the Percent Weight Savings	59
5.	The Effect of $\bar{\lambda}$ on the General Instability Loads.	60
6.	The Effect of $\bar{\lambda}$ on the Percent Weight Savings	61
7.	Initial Post-Buckling Behavior Suggested.	62
8.	Spacing of the Bifurcation Points	63

NOMENCLATURE

Roman Symbols

$A(m)$	mathematical symbol defined by Equation (77).
$A_{ji}, B_{ji}, C_{ji}, D_{ji}$	undetermined coefficients.
A_1, A_2, A_3	coefficients defined by Equations (22).
A_θ, A_ϕ	stiffener cross-sectional areas as shown in Figure 1.
\bar{A}	the amplitude of A_θ and A_ϕ .
a_n, b_n	undetermined coefficients.
$a_{n_{CR}}, b_{n_{CR}}$	the amplitude of the eigenfunctions.
B	coefficient defined by Equation (62).
B_1, B_2, B_3	coefficients defined by Equations (22).
b_θ, b_ϕ	stiffener spacings as shown in Figure 1.
\bar{b}	the amplitude of b_θ and b_ϕ .
C	coefficient defined by Equations (22).
$C_{n_{CR}}, D_{n_{CR}}, E_{n_{CR}}$	coefficients defined by Equations (82).
D	symbol defined by Equation (7).
E	Young's modulus of the shell.
\bar{E}	Young's modulus of the stiffeners.
e	the amplitude of e_θ and e_ϕ .
e_θ, e_ϕ	the stiffener eccentricities as shown in Figure 1.
h	shell thickness.
$h_{equ.}$	equivalent thickness given by Equation (26).
I_θ, I_ϕ	moment of inertia of the stiffeners about their own centroid as shown in Figure 1.

Roman Symbols

\bar{I}	amplitude of I_θ and I_ϕ .
J_E	the strain energy of the shell given by Equation (40).
J_L	the potential energy of the load given by Equation (43).
K	the strain energy per unit area of the undeformed middle-surface given by Equation (39).
$k_{\theta\theta}, k_{\phi\phi}, k_{\theta\phi}$	the changes in curvature and torsion.
$M_\theta, M_\phi, M_{\theta\phi}$	the moment resultants.
$N_\theta, N_\phi, N_{\theta\phi}$	the stress resultants.
n	the mode number.
n_{CR}	the mode number corresponding to the general instability load.
P	the uniform load.
$P[]$	the energy functional given by Equation (63).
P_{CL}	the classical buckling load of an unstiffened spherical shell.
P_{CR}	a critical load.
P_θ, P_ϕ, P_Z	the components of the uniform load in the θ , ϕ , and Z directions.
PWS	percent weight savings given by Equation (32).
$P_m[]$	the sum of all terms in $P[]$ of m th degree in the buckling displacements and their derivatives.
$P_m^i[]$	the coefficient of $(\beta - \beta_{CR})^i$ in the expansion of $P_m[]$.
$P_i(\cos \theta)$	the i th degree Legendre polynomial.
$P_i^j(\cos \theta)$	the associated Legendre polynomial of degree i and order j .
P_{CR}/P_{CL}	a non-dimensional critical load.
$(P_{CR}/P_{CL})_{MIN.}$	the non-dimensional general instability load.

Roman Symbols

R	the radius of the shell.
\bar{S}	the displacement potential given by Equation (53).
S'	the displacement potential given by Equation (14).
u_θ, u_ϕ	the displacements in the θ and ϕ direction.
V	the deformed volume of the shell given by Equation (42).
V_0	the initial volume of the shell.
$W_{IS.}$	the weight of the isotropic shell given by Equation (27).
$W_{SH.}$	the weight of the shell given by Equation (28).
$W_{ST.}$	the weight of the stiffeners given by Equation (30).
$W_{ST.SH.}$	the weight of the stiffened shell given by Equation (31).
W	the deflection in the Z direction.
W_0	the pre-buckling component of W .
W_1	the additional increment in the Z -direction.
X	a variable equal to $\cos \theta$.
Z	the coordinate in the direction of the normal to the shell middle surface as shown in Figure 1.

Greek Symbols

α	the parameter given by Equation (16).
$\alpha_\theta, \alpha_\phi$	the metric coefficients as shown in Figure 1.
β	the parameter given by Equation (16).
$\bar{\beta}$	the parameter given by Equation (44).
$\gamma_{\theta\phi}$	the shearing strain.
δ_{in}	the mathematical symbol given by Equation (A-22).
$\epsilon_{\theta\theta}, \epsilon_{\phi\phi}, \epsilon_{\theta\phi}$	the midsurface strains.

$\epsilon_\theta, \epsilon_\phi, \gamma$	the total strains.
θ, ϕ	the coordinates shown in Figure 1.
$\bar{\lambda}$	the parameter defined by Equation (7).
ν	Poisson's ratio.
ξ_1, \dots, ξ_9	the constants given by Equations (A-1) through (A-9).
ρ	the parameter defined by Equation (7).
ρ_{AV}	the weight of the stiffened shell per unit volume.
ρ_{SH}	the weight per unit volume of the shell.
$\sigma_\theta^{SH}, \sigma_\phi^{SH}, \sigma_{\theta\phi}^{SH}$	the total stresses in the shell.
$\sigma_\theta^{ST}, \sigma_\phi^{ST}, \sigma_{\theta\phi}^{ST}$	the total stresses in the stiffeners.
Φ_θ, Φ_ϕ	the rotations given by Equations (3).

Superscripts

*	term neglected when the Mushtari-Vlasov-Donnell approximation is made.
'	incremental quantities.
0	prebuckling quantities.

Subscripts

CR	corresponding to the critical condition.
i	corresponds to the case of load behavior considered.
0	represents prebuckled quantity.
P	represents the particular solution.

Special Symbols

$(\)_{,\theta}$	the partial derivative with respect to θ .
∇^2	the mathematical operator defined by Equation (16).
$\bar{\nabla}^2$	the mathematical operator defined by Equation (54).

SUMMARY

An analysis of the general instability of eccentrically stiffened complete spherical shells under uniform pressure is presented. The analysis is divided into two parts. The first part is a linear analysis in which the general instability loads and the percent weight savings due to the stiffeners are calculated. The second part is a Koiter-type initial post-buckling analysis in which the imperfection-sensitivity is investigated in an attempt to determine the meaning of the results of the first part when used to predict the general instability loads of imperfect shells.

In this analysis the stiffeners are taken to be one-sided, attached monolithically, placed along the directions of principal curvature, and distributed such that the smeared mass is constant. The following assumptions are made: (i) linear elasticity, (ii) small strains, (iii) moderately small rotations neglecting rotations about the normal, (iv) Kirchhoff Love hypotheses are valid, and (v) the stiffeners are close enough to be smeared. The kinematic relations of Sanders are employed throughout.

In the linear analysis the stress and moment resultants are determined. The principle of the stationary value of the total potential is used to determine the three equilibrium equations. The primary state is determined and used to obtain the three linearized buckling equations. These three equations are reduced to two simplified equations by the introduction of a "displacement potential."

The simplified equations represent an eigenvalue problem in which the eigenfunctions are surface spherical harmonics and the eigenvalues are the general instability loads. From the solution of this eigenvalue problem the effect of load behavior is determined, the effect of making the Mushtari-Vlasov-Donnell approximation is assessed, the non-dimensional general instability loads are calculated, stiffener positioning effects are displayed, and the weight savings due to the stiffeners are determined.

In the initial post-buckling analysis the deflections are assumed to be axisymmetric, the Mushtari-Vlasov-Donnell approximation is made, and only one case of load behavior is considered. The expression for the energy functional is developed. This is expanded twice as shown by Koiter's general theory. The functional is linearized and the eigenvalues and eigenfunctions are determined as in the linear analysis. These eigenvalues and eigenfunctions are substituted into the complete energy functional. The derivative of the functional with respect to the amplitude of the eigenfunctions is then set to zero and the initial post-buckling slope or, when this is zero, the initial post-buckling curvature is calculated. A study of the spacing of the branching points is made. Based on the information from this study in conjunction with the calculated slope or curvature it is shown that the results of this analysis are questionable for some stiffened shells. Parametric studies of the stiffener effects are presented for the other shells.

CHAPTER I

GENERAL INTRODUCTION

Historical Background

The earliest theoretical developments concerned with the general instability* (as opposed to local types of instability discussed in [1]**) of thin stiffened shells [2-4] were based on the assumptions of linear elasticity, small deflections, uniform geometry, and orthotropy. The cylindrical shell and shallow spherical cap were treated.

The importance of the effect of stiffener eccentricity with respect to the shell midsurface was first recognized by Van der Neut [5] in 1947, but it did not become widely known until the late 1950's. Since this time a large number of experimental and theoretical investigations dealing with the eccentricity effect have been reported in the open literature [6-27]. These investigations indicated considerable weight savings and stiffener-positioning effects.

Several of these investigations dealt with stiffened spherical shells. Crawford and Schwartz [13] considered rectangular stiffening on shallow domes. Eccentricity effects were not considered. Bushnell

* A general instability is one in which all the components of the stiffened shell (i.e., the stiffeners and the shell) participate and the deformation extends over the entire surface of the shell.

** Numbers in brackets indicate the references collected in the Bibliography.

[11] used the method of finite differences to solve the general equations of equilibrium for eccentrically stiffened shells of revolution. Complete spherical shells were not considered and parametric studies of the eccentricity effect were not presented.

Some early work with monocoque shells, which had considerable influence on the work with stiffened shells, indicated that the results of the classical linear theory are not sufficient to accurately predict the buckling of thin unstiffened shells.

The buckling of thin cylindrical shells under the action of a uniformly distributed axial load was calculated by R. Lorentz, R. V. Southwell, and others. The same problem was investigated experimentally by E. E. Lundquist and L. H. Donnell. A systematic discrepancy between the theoretically calculated and the experimentally obtained buckling loads was found.

A similar discrepancy was found in the case of the buckling of complete spherical shells under pressure. The theoretical buckling load calculated by R. Zoelly [28], E. Schwerin [29], and A. Van der Neut [30] was $P_{CR} = 2Eh^2/R^2\sqrt{3(1-\nu^2)}$. Some tests made by E. E. Sechler and W. Bollay at the California Institute of Technology, as reported in [31], indicated that the experimental buckling load was only about one fourth of this value.

These disparities between observed and calculated results for buckling loads of unstiffened cylindrical and spherical shells prompted numerous investigations in an attempt to explain them. Of the proposals made in these investigations for causes of the mentioned disparities, the following remain as possibilities: (i) imperfection-sensitivity,

(ii) edge restraint, and (iii) plasticity.

In 1934 Donnell [32] proposed that the discrepancy between experiment and theory is due to imperfections introduced during the manufacture of the test specimens. To analytically account for these imperfections, he extended the "large-deflection" plate equations of von Karman to the analysis of cylindrical shells and used them in an approximate buckling analysis. The solution obtained was later judged to be unsatisfactory by the author himself [33].

A general theory which can provide a first order assessment of imperfection-sensitivity was developed by Koiter [34-36] in 1945. The Koiter-type analysis is rigorous in an asymptotic sense but is valid only in the immediate neighborhood of the bifurcation point. In the development of this theory Koiter investigated states of equilibrium in the neighborhood of the buckling load. He then considered the influence of a small deviation from the perfect geometry. Comparing these results Koiter concluded that a perfect shell which exhibits equilibrium positions in the neighborhood of the buckling load in which the load is smaller than at buckling may be imperfection-sensitive with the severity of the sensitivity indicated by how fast the load decreases in the neighborhood.

Some recent work indicated that the Koiter criterion for determining the imperfection-sensitivity of a shell is necessary but not sufficient. A survey paper by Budiansky and Hutchinson [37] indicated the necessity of the criterion by showing that for all cases reviewed the discrepancies between the test results and theoretically calculated buckling loads were accompanied by implied sensitivity. Hutchinson [38]

showed that the criterion is not sufficient by pointing out that for the oval cylinder a Koiter analysis indicates that the shell is imperfection-sensitive while in reality it is not. Comparison of Koiter's [39] work with that of Pope [40] showed that this is also the case with curved panels.

Koiter-type analyses by Hutchinson [41] considering asymmetric deformations and by Thompson [42] and Walker [43] considering axisymmetric deformations have indicated that unstiffened spherical shells under uniform pressure are imperfection-sensitive.

Experimental verification that geometric imperfections in the specimens are at least partially responsible for the observed disparities between theory and experiment has been provided since 1962. Babcock and Sechler [44], Horton and Durham [45], and others have reported experimental investigations of the behavior of axially compressed cylindrical shells. These investigations were performed upon shells which were accurately fabricated to reduce the influence of imperfections. Buckling loads as high as 90 per cent of the classical value were obtained. Carlson, Sendelbeck, and Hoff [46] performed an experimental investigation of the buckling of complete spherical shells under pressure. These shells were produced by the electroforming process. Extreme care was taken to avoid the introduction of imperfections. Buckling pressures up to 86 per cent of the classical value were obtained.

Edge restraint was mentioned by Donnell [33] as a possible cause of the often found discrepancy between theory and experiment. Although no published record of experiments conducted specifically to determine

the effect of edge restraint upon the buckling process are available, preliminary results obtained at Stanford University [47] indicate that this effect could be appreciable.

The theoretical work which dealt with the edge restraint effect can be divided into two categories. In one of these categories membrane prebuckling deformations were considered and in the other bending. Analyses assuming the existence of a membrane prebuckled state were conducted by Hoff [48], Rehfield [49], and others. Budiansky [50] and later Stein [51] considered a bending prebuckled state. Each of these analyses indicated that the effect of edge restraint on the buckling loads of thin shells can be large. (In the case of the complete spherical shell under uniform load the prebuckled deformation is the uniformly contracted state and the edge restraint effect does not exist.)

Horton and Durham [52] demonstrated experimentally that plasticity can also be a cause of the discrepancy. Mayers and Rehfield [53] formulated the theory and Mayers and Wesenberg [54] furnished an example which demonstrates that plasticity effects can be large.

The possible causes of the discrepancy for unstiffened shells are listed on page 2. The state of affairs is not so clear for stiffened shells. The number of systematic experimental and theoretical investigations of stiffened thin shells which have been reported in the open literature is relatively small. From these it is not even clear whether a systematic discrepancy between experiment and theory exists or not.

Some work has been done on the imperfection-sensitivity of such shells. Crawford and Schwartz [13] made the following statement concerning the imperfection-sensitivity of stiffened shells: ". . . the stability of stiffened shells with their characteristically greater radii of gyration can be expected to be relatively insensitive to initial imperfections. . . ." Some test results on stiffened axially-compressed cylinders, for instance Card's [27], are in fair agreement with the results of the classical theory and thus add substance to Crawford and Schwartz's statement. However, the results of an analysis by Hutchinson and Amazigo [55] which indicates that for certain geometries stiffened cylindrical shells under uniform axial compression are imperfection-sensitive, contradict their statement.

The determination of the effect of load behavior during the buckling process is another problem, independent of the problem of accounting for the discrepancy, which has received some attention in the last few years. The load cases usually considered are (i) the load remains parallel to its original direction, (ii) the load remains perpendicular to the deformed middle surface, and (iii) the load remains directed toward the initial center of curvature.

Boresi [56] considered load cases (i) and (ii) for a thin circular ring under uniformly distributed radial load. Armenakas and Herrmann [57] considered these same cases for long cylinders under lateral pressure. Smith and Simites [58] considered all three cases for circular rings.

Recently Simites and Cole [59] considered all three cases for the unstiffened complete spherical shell under uniform pressure. The

buckling load was found to be independent of load behavior. Koiter [60] showed that the buckling load of any thin shell which buckles into a large number of waves is independent of load behavior.

Only a few references which would illustrate the development and the present state of knowledge in the pertinent areas have been presented here. Additional references dealing with specific points of interest are presented where needed throughout the thesis. For additional references see Fung and Sechler [61], Hoff [48,62], and Budiansky and Hutchinson [37].

Scope of the Analysis

The work reported in this dissertation can be conveniently divided into two chapters, each of which is complete within itself.

In Chapter II a buckling analysis of eccentrically stiffened complete thin spherical shells under uniform load considering asymmetric deformations is presented. The analysis is based on the following assumptions: (i) linear elasticity, (ii) small strains, (iii) moderately small rotations neglecting rotations about the normal, (iv) Kirchhoff-Love hypotheses are valid, and (v) that the stiffeners are close enough to be smeared. The stiffeners are taken to be one-sided, attached monolithically, placed along the directions of principal curvature, and distributed such that the smeared mass is constant. The three cases of load behavior previously mentioned are considered, the effect of making the Mushtari-Vlasov-Donnell approximation is assessed, the non-dimensional general instability loads are calculated,

stiffener positioning effects are displayed, and the weight savings due to the stiffeners are determined.

In Chapter III a Koiter-type initial post-buckling analysis of the eccentrically stiffened shells that were treated in Chapter II considering only axisymmetric deformations is presented in an attempt to determine their imperfection-sensitivity. The analysis is based on the same assumptions that were made in Chapter II but the non-linear terms are retained. Only load behavior case (ii) is considered and the Mushtari-Vlasov-Donnell approximation is made throughout. The initial post-buckling slopes are calculated and when these are zero the initial post-buckling curvatures are examined. A study of the spacing of the branching points is made. From this study it was determined that the meaning of the results is questionable for shells which have closely spaced branching points. A parametric study of the imperfection-sensitivity of the shells for which the results of the initial post-buckling analysis can be expected to have meaning is presented.

CHAPTER II

LINEAR ANALYSIS

Introductory Remarks

Some early experimental work [3,63-65] indicated that the buckling loads of complete thin unstiffened spherical shells under uniform load were much smaller than predicted by the classical linear theory and thus cast doubt upon the applicability of this theory to the buckling of such shells. This doubt, however, was recently dispelled by the experimental work of Carlson, Sendelbeck, and Hoff [46]. They obtained experimental buckling loads of up to 86 per cent of the classical value for such shells.

The stability of eccentrically stiffened spherical shells has been studied in reference [3,11,13,15].

In reference [15] Ebner used an approximate method to calculate the general instability loads of uniformly pressurized, meridionally stiffened, shallow spherical domes. He did not account for stiffener eccentricity. Tests were performed but the stiffener geometry was not presented.

In reference [3] Klöppel and Jungbluth derived a semi-empirical expression for the buckling loads of stiffened spherical caps. The effect of the stiffeners was included through the introduction of equivalent bending and extensional rigidities into a formula for the

buckling pressure of a monocoque shell. The eccentricity effect was not considered. Test results were inconsistent.

In reference [13] Crawford and Schwartz calculated bifurcation loads for grid-stiffened spherical domes. They idealized the structure by considering it to be orthotropic and by neglecting the eccentricity of the stiffeners.

In reference [11] Bushnell set up the general equations governing the stability of shells of revolution. He solved the equations using the method of finite differences for, among other geometries, the internally stiffened spherical cap. He did consider eccentricity effects, but did not present parametric studies of these effects.

In this chapter the general-instability of eccentrically stiffened complete thin spherical shells is investigated. The analysis is based on a small strain linearly elastic theory. The stiffeners are taken to be one-sided, attached monolithically, placed along the directions of principal curvature and distributed such that the smeared mass is constant. No restriction is placed on the kinematic behavior of the shell during buckling. Three cases of load behavior are considered, the effect of making the Mushtari-Vlasov-Donnell approximation is assessed, the weight savings are computed, and parametric studies of the eccentricity effects are presented. The critical condition obtained is shown to coincide with that obtained in [59] when the parameters which characterize the stiffeners ($e/h, \bar{\lambda}, \rho$) are set to zero.

Formulation of the Problem

The thin spherical shell is eccentrically stiffened along directions of principal curvature such that (i) the stiffeners are both on the same side with spacings characterized by $\theta = \text{constant}$ and $\phi = \text{constant}$, (ii) the stiffener eccentricity is the same for all stiffeners and constant, and (iii) the smeared extensional and flexural stiffnesses are the same along both directions and constant. Assumptions (ii) and (iii) are associated with the conjecture that the smeared mass of the closely spaced stiffeners must be constant in order to resist a constant pressure efficiently.

The kinematic relations derived by Sanders [66] are employed in the present theoretical development. These relations are based on the assumptions of small strains and rotations neglecting rotations about the normal. The geometry and sign convention are given in Figure 1. The shell mid-surface is taken to be the reference surface. The kinematic relations are

$$\epsilon_{\theta\theta} = \frac{1}{R} (u_{\theta,\theta} + W) + \frac{1}{2} \phi_{\theta}^2 \quad (1a)$$

$$\epsilon_{\phi\phi} = \frac{1}{R} (u_{\phi,\phi} \csc\theta + u_{\theta} \cot\theta + W) + \frac{1}{2} \phi_{\phi}^2 \quad (1b)$$

$$\gamma_{\theta\phi} = 2\epsilon_{\phi\theta} = \frac{1}{R} (u_{\phi,\theta} + u_{\theta,\phi} \csc\theta - u_{\phi} \cot\theta) + \phi_{\phi} \phi_{\theta} \quad (1c)$$

$$K_{\theta\theta} = \frac{1}{R} \phi_{\theta,\theta} \quad (2a)$$

$$k_{\phi\phi} = \frac{1}{R} (\phi_{\phi,\phi} \csc \theta + \phi_{\theta} \cot \theta) \quad (2b)$$

$$k_{\theta\phi} = \frac{1}{2R} (\phi_{\phi,\theta} + \phi_{\theta,\phi} \csc \theta - \phi_{\phi} \cot \theta) \quad (2c)$$

$$\phi_{\theta} = \frac{1}{R} (u_{\theta}^{*} - W_{,\theta}) \quad (3a)$$

$$\phi_{\phi} = \frac{1}{R} (u_{\phi}^{*} - W_{,\phi} \csc \theta) \quad (3b)$$

where the "comma" denotes partial differentiation with respect to the subscripts that follow, and the "star" terms in the expressions for the rotations are dropped in the Mushtari-Vlasov-Donnell approximation.

The stiffener-shell connection is assumed to be monolithic and the Kirchhoff-Love hypotheses are assumed to be valid for the combination. According to this the strains of any material point are given by

$$\epsilon_{\theta} = \epsilon_{\theta\theta} + z k_{\theta\theta} \quad (4a)$$

$$\epsilon_{\phi} = \epsilon_{\phi\phi} + z k_{\phi\phi} \quad (4b)$$

$$\gamma = \gamma_{\theta\phi} + 2z k_{\theta\phi} \quad (4c)$$

If the material on or before loss of stability is linearly elastic and the Poisson effect for the stiffeners is neglected, then the mathematical expression of Hooke's law becomes

$$\sigma_{\theta}^{sh} = \frac{E}{1 - \nu^2} (\epsilon_{\theta} + \nu \epsilon_{\phi}) \quad (5a)$$

$$\sigma_{\phi}^{sh} = \frac{E}{1 - \nu^2} (\epsilon_{\phi} + \nu \epsilon_{\theta}) \quad (5b)$$

$$\sigma_{\theta\phi}^{sh} = \frac{E}{2(1+\nu)} \gamma \quad (5c)$$

$$\sigma_{\theta}^{st} = \bar{E} \epsilon_{\theta} \quad (5d)$$

$$\sigma_{\phi}^{st} = \bar{E} \epsilon_{\phi} \quad (5e)$$

$$\sigma_{\theta\phi}^{st} = \frac{\bar{E}}{2} \gamma \quad (5f)$$

Note that both stiffeners are made out of the same material.

Integrating the stresses in the usual manner in order to obtain stress and moment resultants, and using assumptions (i) through (iii) for the closely spaced stiffeners, the constitutive equations are (see Figure 1)

$$N_{\theta} = \frac{Eh}{1 - \nu^2} [(1+\bar{\lambda})\epsilon_{\theta\theta} + \nu\epsilon_{\phi\phi} + e\bar{\lambda}k_{\theta\theta}] \quad (6a)$$

$$N_{\phi} = \frac{Eh}{1 - \nu^2} [(1+\bar{\lambda})\epsilon_{\phi\phi} + \nu\epsilon_{\theta\theta} + e\bar{\lambda}k_{\phi\phi}] \quad (6b)$$

$$N_{\theta\phi} = N_{\phi\theta} = \frac{Eh}{1 - \nu^2} [(1+\bar{\lambda}-\nu)\epsilon_{\theta\phi} + e\bar{\lambda}k_{\theta\phi}] \quad (6c)$$

$$M_{\theta} = D[(1+\rho)k_{\theta\theta} + \nu k_{\phi\phi}] + \frac{Eh}{1-\nu^2} \bar{\lambda}e[\epsilon_{\theta\theta} + ek_{\theta\theta}] \quad (6d)$$

$$M_{\phi} = D[(1+\rho)k_{\phi\phi} + \nu k_{\theta\theta}] + \frac{Eh}{1-\nu^2} \bar{\lambda}e[\epsilon_{\phi\phi} + ek_{\phi\phi}] \quad (6e)$$

$$M_{\theta\phi} = M_{\phi\theta} = D(1+\rho-\nu)k_{\theta\phi} + \frac{Eh}{1-\nu^2} \bar{\lambda}e[\epsilon_{\theta\phi} + ek_{\theta\phi}] \quad (6f)$$

where

$$\bar{\lambda} = (1-\nu^2) \frac{\bar{E}\bar{A}}{Eh \bar{b}}; \quad \rho = \frac{\bar{E}\bar{I}}{D\bar{b}}; \quad D = \frac{Eh^3}{12(1-\nu^2)}. \quad (7)$$

Use of the principle of the stationary value of the total potential leads to the three equilibrium equations.

$$\begin{aligned} R[(N_{\theta} \sin \theta)_{,\theta} + N_{\theta\phi,\phi} - N_{\phi} \cos \theta] + (M_{\theta}^{*} \sin \theta)_{,\theta} + M_{\theta\phi,\phi}^{*} \\ - M_{\phi}^{*} \cos \theta - R \sin \theta (N_{\theta}^{*} \phi_{\theta} + N_{\theta\phi}^{*} \phi_{\phi}) + P_{\theta} R^2 \sin \theta = 0 \end{aligned} \quad (8a)$$

$$\begin{aligned} R[N_{\phi,\phi} + (N_{\theta\phi} \sin \theta)_{,\theta} + N_{\theta\phi} \cos \theta] + M_{\phi,\phi}^{*} + (M_{\theta\phi}^{*} \sin \theta)_{,\theta} \\ + M_{\theta\phi}^{*} \cos \theta - R \sin \theta (N_{\phi}^{*} \phi_{\phi} + N_{\theta\phi}^{*} \phi_{\theta}) + P_{\phi} R^2 \sin \theta = 0 \end{aligned} \quad (8b)$$

$$[(M_{\theta} \sin \theta)_{,\theta} + M_{\theta\phi,\phi} - M_{\phi} \cos \theta]_{,\theta} + \csc \theta [M_{\phi,\phi} + (M_{\theta\phi} \sin \theta)_{,\theta}$$

* These terms are dropped under the Mushtari-Vlasov-Donnell approximation.

$$\begin{aligned}
& + M_{\theta\phi} \cos \theta]_{,\phi} - R \sin \theta (N_{\phi} + N_{\theta}) - R [\sin \theta (N_{\theta}\phi_{\theta} + N_{\theta\phi}\phi_{\phi})]_{,\theta} \\
& - R [N_{\phi}\phi_{\phi} + N_{\theta\phi}\phi_{\theta}]_{,\phi} + P_Z R^2 \sin \theta = 0. \quad (8c)
\end{aligned}$$

Buckling Analysis

It can be easily confirmed that the primary state (unbuckled state) which satisfies the equilibrium equations, Equations (8), is characterized by the following:

$$W^0 = PR^2(1-\nu^2)/2Eh(1+\bar{\lambda}+\nu); \quad u_{\theta}^0 = u_{\phi}^0 = 0 \quad (9a)$$

$$\phi_{\theta}^0 = \phi_{\phi}^0 = 0 \quad (9b)$$

$$P_{\theta}^0 = P_{\phi}^0 = 0; \quad P_Z^0 = P \quad (9c)$$

$$N_{\theta}^0 = N_{\phi}^0 = PR/2; \quad N_{\theta\phi}^0 = 0 \quad (9d)$$

$$M_{\theta}^0 = M_{\phi}^0 = PR\bar{\lambda}e/2(1+\bar{\lambda}+\nu); \quad M_{\theta\phi}^0 = 0 \quad (9e)$$

According to the adjacent equilibrium criterion of instability (in which the existence of a bifurcation point is assumed) the following conditions are assumed to exist:

$$W = P_{CR} R^2(1-\nu^2)/2Eh(1+\bar{\lambda}+\nu) + W'; \quad u_{\theta} = u'_{\theta}; \quad u_{\phi} = u'_{\phi} \quad (10a)$$

$$\Phi_{\theta} = \Phi'_{\theta}; \quad \Phi_{\phi} = \Phi'_{\phi} \quad (10b)$$

$$P_{\theta} = P'_{\theta}; \quad P_{\phi} = P'_{\phi}; \quad P_Z = P_{CR} + P'_Z \quad (10c)$$

$$N_{\theta} = P_{CR} R/2 + N'_{\theta}; \quad N_{\phi} = P_{CR} R/2 + N'_{\phi}; \quad N_{\theta\phi} = N'_{\theta\phi} \quad (10d)$$

$$M_{\theta} = P_{CR} R \bar{\lambda} e / 2(1 + \bar{\lambda} + \nu) + M'_{\theta}; \quad M_{\phi} = P_{CR} R \bar{\lambda} e / 2(1 + \bar{\lambda} + \nu) + M'_{\phi} \quad (10e)$$

$$M_{\theta\phi} = M'_{\theta\phi} \quad (10f)$$

where the "primed" quantities represent the increments which take the system from the unbuckled state to the adjacent buckled equilibrium state.

Substitution of Equations (10) into Equations (8) and linearization gives the buckling equations which follow:

$$R[\cos \theta (N'_{\theta} - N'_{\phi}) + \sin \theta N'_{\theta,\theta} + N'_{\theta\phi,\phi} - \frac{1}{2} P_{CR}^* R \sin \theta \Phi'_{\theta}] \quad (11a)$$

$$+ \cos \theta (M_{\theta}^{**'} - M_{\phi}^{*'}) + \sin \theta M_{\theta,\theta}^{*'} + M_{\theta\phi,\phi}^{*'} + R^2 \sin \theta P'_{\theta} = 0$$

$$R[N'_{\phi,\phi} + 2 \cos \theta N'_{\theta\phi} + \sin \theta N'_{\theta\phi,\theta} - \frac{1}{2} P_{CR}^* R \sin \theta \Phi'_{\phi}] + M_{\phi,\phi}^{*'} \quad (11b)$$

$$+ 2 \cos \theta M_{\theta\phi}^{*'} + \sin \theta M_{\theta\phi,\theta}^{*'} + R^2 \sin \theta P'_{\phi} = 0 \quad (11b)$$

$$- R \sin \theta (N'_\theta + N'_\phi) + [\cos \theta (M'_\theta - M'_\phi) + \sin \theta M'_{\theta,\theta} + M'_{\theta\phi,\phi}],_\theta \quad (11c)$$

$$+ \csc \theta [M'_{\phi,\phi} + 2 \cos \theta M'_{\theta\phi} + \sin \theta M'_{\theta\phi,\theta}],_\phi + \frac{1}{2} P_{CR}^R [\sin \theta \phi'_{\theta,\theta} + \cos \theta \phi'_\theta + \phi'_{\phi,\phi}] + R^2 \sin \theta P'_Z = 0$$

where the stress and moment resultants are the same as in Equations (6) with ϵ_θ , ϵ_ϕ , and $\epsilon_{\theta\phi}$ replaced by

$$\epsilon'_{\theta\theta} = \frac{1}{R} (u'_{\theta,\theta} + W') \quad (12a)$$

$$\epsilon'_{\phi\phi} = \frac{1}{R} (u'_{\phi,\phi} \csc \theta + u'_\theta \cot \theta + W') \quad (12b)$$

$$\epsilon'_{\theta\phi} = \frac{1}{2R} (u'_{\phi,\theta} + u'_{\theta,\phi} \csc \theta - u'_\theta \cot \theta) \quad (12c)$$

and all the other primed quantities are the same as shown previously with u_θ , u_ϕ , and W replaced by u'_θ , u'_ϕ , and W' , respectively.

The effect of load behavior is introduced into the buckling equations by substituting appropriate expression for P'_θ , P'_ϕ , and P'_Z . The cases of load behavior considered here are (i) the load remains parallel to its original direction, (ii) the load remains perpendicular to the deformed middle surface, and (iii) the load remains directed toward the initial center of curvature. The cases are indicated with braces as shown below

$$\begin{pmatrix} \text{Case (i)} \\ \text{Case (ii)} \\ \text{Case (iii)} \end{pmatrix}$$

As seen by geometrical considerations the loading components to be introduced into the buckling equations are as follows:

$$P'_{\theta} = \frac{P_{CR}}{R} \begin{pmatrix} 0 \\ u'_{\theta} - w'_{,\theta} \\ u'_{\theta} \end{pmatrix} \quad (13a)$$

$$P'_{\phi} = \frac{P_{CR}}{R} \begin{pmatrix} 0 \\ u'_{\phi} - \csc \theta w'_{,\phi} \\ u'_{\phi} \end{pmatrix} \quad (13b)$$

$$P'_Z = \begin{pmatrix} 0 \\ 0 \\ 0 \end{pmatrix} . \quad (13c)$$

If, in addition to Equations (13), a displacement potential, S' , such that

$$u'_{\theta} = S'_{,\theta} \quad (14a)$$

$$u'_{\phi} = S'_{,\phi} \csc \theta \quad (14b)$$

is introduced into Equations (11), the buckling equations take the following form:

$$\sin \theta \frac{\partial}{\partial \theta} \left(\{-\bar{\lambda} \frac{e}{R} + \alpha^*(1+\rho) + \bar{\lambda} \frac{e^{2*}}{R^2}\} \nabla^2 + [1 + v + \bar{\lambda}(1 - \frac{e}{R} + \frac{e^*}{R}) \right. \quad (15a)$$

$$\left. - \alpha^*(1+\rho-v) - \bar{\lambda} \frac{e^{2*}}{R^2} + \beta \begin{pmatrix} 1^* \\ 1^* - 2 \\ 1^* \end{pmatrix} \right] W' + \{[1+\bar{\lambda}(1 + \frac{e}{R} + \frac{e^*}{R})$$

$$+ \alpha^*(1+\rho) + \bar{\lambda} \frac{e^{2*}}{R^2}\} \nabla^2 + [1-v+\bar{\lambda}(1 + \frac{e}{R} + \frac{e^*}{R}) + \alpha^*(1+\rho-v)$$

$$+ \bar{\lambda} \frac{e^{2*}}{R^2} - \beta \begin{pmatrix} 1^* \\ 1^* - 2 \\ 1^* - 2 \end{pmatrix} \right] S') = 0$$

$$\frac{\partial}{\partial \phi} \left(\{-\bar{\lambda} \frac{e}{R} + \alpha^*(1+\rho) + \bar{\lambda} \frac{e^{2*}}{R^2}\} \nabla^2 + [1+v+\bar{\lambda}(1 - \frac{e}{R} + \frac{e^*}{R}) \right. \quad (15b)$$

$$\left. - \alpha^*(1+\rho-v) - \bar{\lambda} \frac{e^{2*}}{R^2} + \beta \begin{pmatrix} 1^* \\ 1^* - 2 \\ 1^* \end{pmatrix} \right] W' + \{[1+\bar{\lambda}(1 + \frac{e}{R} + \frac{e^*}{R})$$

$$+ \alpha^*(1+\rho) + \bar{\lambda} \frac{e^{2*}}{R^2}\} \nabla^2 + [1-v+\bar{\lambda}(1 + \frac{e}{R} + \frac{e^*}{R}) + \alpha^*(1+\rho-v)$$

$$+ \bar{\lambda} \frac{e^{2*}}{R^2} - \beta \begin{pmatrix} 1^* \\ 1^* - 2 \\ 1^* - 2 \end{pmatrix} \right] S') = 0$$

$$\{-[\alpha(1+\rho) + \bar{\lambda} \frac{e^2}{R^2}] \nabla^4 - [\alpha(1+\rho-v) - 2\bar{\lambda} \frac{e}{R} + \bar{\lambda} \frac{e^2}{R^2} - \beta] \nabla^2 \quad (15c)$$

$$- 2(1+\bar{\lambda}+v)\} W' + \{[\bar{\lambda} \frac{e}{R} + \alpha^*(1+\rho) + \bar{\lambda} \frac{e^{2*}}{R^2}] \nabla^4 - [1+v$$

$$+ \bar{\lambda} \left(1 - \frac{e}{R} + \frac{e^*}{R}\right) - \alpha^* (1+\rho-v) - \bar{\lambda} \frac{e^{2*}}{R^2} + \beta \nabla^2 \} S' = 0$$

where

$$\alpha = \frac{1}{12} (h/R)^2 \quad (16a)$$

$$\beta = P_{CR} R(1-v^2)/2Eh \quad (16b)$$

$$\nabla^2 = \csc^2 \theta \frac{\partial^2}{\partial \phi^2} + \cot \theta \frac{\partial}{\partial \theta} + \frac{\partial^2}{\partial \theta^2} \quad (16c)$$

At first it may seem that the introduction of the displacement potential overconstrains the problem. This is not the case, however, since the first two of Equations (15) are seen to be satisfied by the same condition.

If Equation (15a) is divided by $\sin \theta$ and integrated with respect to θ and Equation (15b) is integrated with respect to ϕ , these two equations can be reduced to the following single equation:

$$\{-[\bar{\lambda} \frac{e}{R} + \alpha^* (1+\rho) + \bar{\lambda} \frac{e^{2*}}{R^2}] \nabla^2 + [1+v+\bar{\lambda} (1 - \frac{e}{R} + \frac{e^*}{R}) \quad (17)$$

$$- \alpha^* (1+\rho-v) - \bar{\lambda} \frac{e^{2*}}{R^2} + \beta \begin{pmatrix} 1^* \\ 1^* - 2 \\ 1^* \end{pmatrix} \} W' + \{ [1 + \bar{\lambda} (1 + \frac{e}{R} + \frac{e^*}{R})$$

$$+ \alpha^* (1+\rho) + \bar{\lambda} \frac{e^{2*}}{R^2}] \nabla^2 + [1-v+\bar{\lambda} (1 + \frac{e}{R} + \frac{e^*}{R}) + \alpha^* (1+\rho-v)$$

$$+ \bar{\lambda} \frac{e^{2*}}{R^2} - \beta \begin{pmatrix} 1^* \\ 1^* - 2 \\ 1^* - 2 \end{pmatrix}] S' = C$$

The buckling equations are now Equations (15c) and (17).

The particular solution to this system of Equations [Equations (15c) and (17)] can be shown to be

$$W'_P = 0 \quad (18a)$$

$$S'_P = C/[1-v+\bar{\lambda}(1 + \frac{e}{R} + \frac{e^*}{R}) + \alpha^*(1+\rho-v) + \bar{\lambda} \frac{e^{2*}}{R^2} - \beta \begin{pmatrix} 1^* \\ 1^* - 2 \\ 1^* - 2 \end{pmatrix}]. \quad (18b)$$

However, since the values of u'_θ and u'_ϕ are not altered, as seen from Equations (14), by the addition of a constant to S' , C may be set equal to zero.

The buckling equations thus become

$$\{-[\bar{\lambda} \frac{e}{R} + \alpha^*(1+\rho) + \bar{\lambda} \frac{e^{2*}}{R^2}]\nabla^2 + [1+v+\bar{\lambda}(1 - \frac{e}{R} + \frac{e^*}{R}) - \alpha^*(1+\rho-v) \quad (19a)$$

$$- \bar{\lambda} \frac{e^{2*}}{R^2} + \beta \begin{pmatrix} 1^* \\ 1^* - 2 \\ 1^* \end{pmatrix}] W' + \{[1 + \bar{\lambda}(1 + \frac{e}{R} + \frac{e^*}{R}) + \alpha^*(1+\rho)$$

$$+ \bar{\lambda} \frac{e^{2*}}{R^2}]\nabla^2 + [1-v+\bar{\lambda}(1 + \frac{e}{R} + \frac{e^*}{R}) + \alpha^*(1+\rho-v) + \bar{\lambda} \frac{e^{2*}}{R^2}$$

$$- \beta \begin{pmatrix} 1^* \\ 1^* - 2 \\ 1^* - 2 \end{pmatrix} S' = 0$$

$$\begin{aligned} & \{-[\alpha(1+\rho) + \bar{\lambda} \frac{e^2}{R^2}]v^4 - [\alpha(1+\rho-v) - 2\bar{\lambda} \frac{e}{R} + \bar{\lambda} \frac{e^2}{R^2} - \beta]v^2 \\ & - 2(1+\bar{\lambda}+v)\}W' + \{[\bar{\lambda} \frac{e}{R} + \alpha^*(1+\rho) + \bar{\lambda} \frac{e^{2*}}{R^2}]v^4 - [1+v+\bar{\lambda}(1 - \frac{e}{R} + \frac{e^*}{R}) \\ & - \alpha^*(1+\rho-v) - \bar{\lambda} \frac{e^{2*}}{R^2} + \beta^*]v^2\}S' = 0 \end{aligned} \quad (19b)$$

The problem has thus been reduced to an eigenvalue problem. The eigenfunctions of this problem are surface spherical harmonics. Thus W' and S' are taken in the form which follows:

$$W' = \sum_{i=0}^{\infty} A_{0i} P_i(\cos \theta) + \sum_{i=1}^{\infty} \sum_{j=1}^i [A_{ji} \cos j\phi + B_{ji} \sin j\phi] P_i^j(\cos \theta) \quad (20a)$$

$$S' = \sum_{i=0}^{\infty} C_{0i} P_i(\cos \theta) + \sum_{i=1}^{\infty} \sum_{j=1}^i [C_{ji} \cos j\phi + D_{ji} \sin j\phi] P_i^j(\cos \theta) \quad (20b)$$

As shown in Appendix A, substitution of Equations (20) into the buckling Equations (19) shows that the consideration of axisymmetric deflections would have been sufficient for this analysis and leads to the following relation from which the eigenvalues (non-dimensional critical loads, P_{CR}/P_{CL}) of the problem can be obtained:

$$A_i (P_{CR}/P_{CL})^2 + B_i (P_{CR}/P_{CL}) + C = 0 \quad (21)$$

In Equation (21) the subscript "i" refers to the load case considered and $P_{CL} = -2E(h/R)^2/\sqrt{3(1-\nu^2)}$ is the classical buckling load for the unstiffened shell. The constants in the equation are as follows:

$$A_1 = 0 \quad (22a)$$

$$A_2 = -1^* + 1 \quad (22b)$$

$$A_3 = 1 \quad (22c)$$

$$B_1 = \frac{1}{2} \left[\frac{1}{3}(1-\nu^2) \right]^{-1/2} \left(\frac{R}{h} \right) \{ [1 + \bar{\lambda}(1 + \frac{e}{R} - \frac{e^*}{R})]n(n+1) - [1 + 2^* - \nu + 2\nu^* + \bar{\lambda}(1 + 2^* + \frac{e}{R} - \frac{e^*}{R})] - 2(1+\bar{\lambda}+\nu)/n(n+1) \} \quad (22d)$$

$$B_2 = \frac{1}{2} \left[\frac{1}{3}(1-\nu^2) \right]^{-1/2} \left(\frac{R}{h} \right) \{ [1 + \bar{\lambda}(1 + 3\frac{e}{R} - \frac{e^*}{R}) + 2\alpha(1+\rho)(1^*-1) \} \quad (22e)$$

$$+ 2\bar{\lambda} \frac{e^2}{R^2} (1^*-1)]n(n+1) + [1 - 2^* + 3\nu - 2\nu^* + \bar{\lambda}(1 - 2^* - 7\frac{e}{R}$$

$$+ 3\frac{e^*}{R}) + 2(\alpha-\alpha^*)(1+\rho-\nu) + 2\bar{\lambda} \frac{e^2}{R^2} (1-1^*) + (-2^*+4)(1+\bar{\lambda}+\nu)/n(n+1) \}$$

$$B_3 = \frac{1}{2} \left[\frac{1}{3}(1-\nu^2) \right]^{-1/2} \left(\frac{R}{h} \right) \{ [1 + \bar{\lambda}(1 + \frac{e}{R} - \frac{e^*}{R}) - 2\alpha(1+\rho) - 2\bar{\lambda} \frac{e^2}{R^2}]n(n+1)$$

$$- [1 + 2^* - \nu + 2\nu^* + \bar{\lambda}(1 + 2^* + 5\frac{e}{R} - \frac{e^*}{R} - 2\alpha(1+\rho-\nu) - 2\bar{\lambda} \frac{e^2}{R^2}]$$

$$+ (-2^{**}+4)(1+\bar{\lambda}+\nu)/n(n+1)\} \quad (22f)$$

$$\begin{aligned} C = & \frac{3}{2(1-\nu^2)} (R/h)^2 \{ -[\alpha(1+\rho)+\bar{\lambda} \frac{e^2}{R^2}]n(n+1) + [\alpha(1+\rho-\nu) \\ & - 2\bar{\lambda} \frac{e}{R} + \bar{\lambda} \frac{e^2}{R^2}] - 2(1+\bar{\lambda}+\nu)/n(n+1) \} ([1 + \bar{\lambda}(1 + \frac{e}{R} + \frac{e^{**}}{R}) \\ & + \alpha^{**}(1+\rho) + \bar{\lambda} \frac{e^{2*}}{R^2}]n(n+1) - [1-\nu+\bar{\lambda}(1 + \frac{e}{R} + \frac{e^{**}}{R}) + \alpha^{**}(1+\rho-\nu) \\ & + \bar{\lambda} \frac{e^{2*}}{R^2}]) + ([\bar{\lambda} \frac{e}{R} + \alpha^{**}(1+\rho) + \bar{\lambda} \frac{e^{2*}}{R^2}]n(n+1) + [1 + \nu + \bar{\lambda}(1 - \frac{e}{R} \\ & + \frac{e^{**}}{R}) - \alpha^{**}(1+\rho-\nu) - \bar{\lambda} \frac{e^{2*}}{R^2}]^2 \} \end{aligned} \quad (22g)$$

From Equation (21) it is seen that

$$(P_{CR}/P_{CL})_i = (-B_i + \sqrt{B_i^2 - 4A_i C})/2A_i \quad (23)$$

when $A_i \neq 0$, and that

$$(P_{CR}/P_{CL})_i = -C/B_i \quad (24)$$

when $A_i = 0$.

For a given geometry, Equations (23) and (24) give the non-dimensional critical loads, P_{CR}/P_{CL} , as a function of n only. The non-dimensional general instability loads $(P_{CR}/P_{CL})_{MIN}$ are then obtained by minimization of these relations with respect to integer values of n .

Note that when the parameters which characterize the stiffeners, e/h , $\bar{\lambda}$, and ρ , are set to zero the critical condition, Equation (21), reduces to that of the unstiffened shell as given by Equation (15) of reference [59].

Weight Savings

An indication of the weight savings due to the stiffeners is obtained by comparing the weight of an isotropic spherical shell which has the same critical load as the stiffened shell to the weight of the stiffened shell.

Before the weight of the isotropic or unstiffened shell can be obtained an equivalent thickness, h_{equ} , must be found. To determine the equivalent thickness solve the equation

$$2E(h_{\text{equ}}/R)^2/\sqrt{3(1-\nu^2)} = (P_{\text{CR}})_{\text{MIN.}} \quad (25)$$

for h_{equ} . This results in the relation

$$h_{\text{equ.}} = h\sqrt{(P_{\text{CR}}/P_{\text{CL}})_{\text{MIN.}}} \quad (26)$$

The weight of the isotropic shell is then easily determined as

$$W_{\text{IS.}} = 4\pi R^2 h \rho_{\text{AV}} \sqrt{(P_{\text{CR}}/P_{\text{CL}})_{\text{MIN.}}} \quad (27)$$

where the average density, ρ_{AV} , is the weight of the stiffened shell per unit volume.

The weight of the stiffened shell can be considered as the weight of the shell, $W_{SH.}$, plus the weight of the stiffeners, $W_{ST.}$. The weight of the shell is given by

$$W_{SH.} = 4\pi R^2 h \rho_{SH.} \quad (28)$$

The weight of the stiffeners is obtained by computing the volume of each stiffener and then multiplying this by the density and the number of stiffeners. Thus the weight of the stiffeners is

$$W_{ST.} = \rho_{ST.} \left[\int_0^\pi \int_{-\pi}^\pi \frac{\bar{A} R}{\bar{b}(R+e)} (R+e)^2 \sin \theta \, d\theta \, d\phi \right. \quad (29)$$

$$\left. + \frac{2\pi R}{\bar{b}} \int_0^\pi (R+e) \bar{A} \sin \theta \, d\theta \right]$$

or

$$W_{ST.} = 4\pi R^2 h \rho_{ST.} \left[\frac{2E}{\bar{E}(1-\nu^2)} \bar{\lambda} \left(1 + \frac{e}{R}\right) \right]. \quad (30)$$

The weight of the stiffened shell can thus be written as

$$W_{ST.SH.} = 4\pi R^2 h \rho_{SH.} \left[1 + \frac{\rho_{ST.}}{\rho_{SH.}} \frac{2E}{\bar{E}(1-\nu^2)} \bar{\lambda} \left(1 + \frac{e}{R}\right) \right]. \quad (31)$$

Once the weights of the isotropic shell and the stiffened shell are known the percentage weight savings due to the stiffeners can be found from the relation

$$PWS = [1 - (W_{ST.SH.}/W_{IS.})]100. \quad (32)$$

Discussion and Conclusions

The results of this analysis were obtained by making a numerical study of the critical condition given by Equation (21). In making this study two computer programs were written for the Univac 1108. In one of these the Mushtari-Vlasov-Donnell approximation was made and in the other it was not. Throughout the numerical work the values $\nu = 1/3$ and $\rho_{ST.}/\rho_{SH.} = 1$ were used. These programs are contained in Appendix B.

Table 1 contains some typical output from each of these programs. From this table the effect of making the Mushtari-Vlasov-Donnell approximation was assessed and the effect of the cases of load behavior considered was determined.

In Figure 2 the non-dimensional general instability loads, $(P_{CR}/P_{CL})_{MIN.}$, and the percentage weight savings, PWS, due to the stiffeners are presented as functions of the non-dimensional stiffener eccentricity, e/h , for typical shells with light, moderate, and heavy stiffening. From this figure a parametric study of the effect of e/h on $(P_{CR}/P_{CL})_{MIN.}$ and PWS was made.

From Figures 3 through 6 a parametric study of the effects which the remaining non-dimensional stiffener parameters, $\bar{\lambda}$ and ρ , have on $(P_{CR}/P_{CL})_{MIN.}$ and PWS was made.

A careful examination of the results of this analysis leads to the following conclusions regarding the buckling of the eccentrically stiffened complete spherical shells considered here:

1. The assumption of axisymmetric kinematic behavior leads to the same critical loads (note that the results of Chapter II are independent of this assumption).
2. The Mushtari-Vlasov-Donnell approximation does not appreciably affect either the general instability loads or the failure modes.
3. The effect of load behavior during buckling is negligibly small.
4. Inside stiffeners lead to a stronger configuration than outside stiffeners.
5. Increasing $|e/h|$ increases $(P_{CR}/P_{CL})_{MIN.}$.
6. Increasing $\bar{\lambda}$ increases $(P_{CR}/P_{CL})_{MIN.}$ but decreases PWS.
7. In order to sustain a given uniformly distributed pressure the isotropic shell must be heavier than the stiffened shell.

CHAPTER III

AXISYMMETRIC INITIAL POST-BUCKLING ANALYSIS

Introductory Remarks

In Chapter II the general instability loads of perfectly formed eccentrically stiffened complete spherical shells under uniform load are calculated. The meaning of these loads when applied to imperfectly formed shells is not clear. To clarify this meaning the imperfection-sensitivity of the shells is determined. For shells which are imperfection-sensitive these loads can be thought of as upper bounds on the actual loads, and the difference between the calculated and actual loads can be expected to decrease as the imperfection-sensitivity decreases.

Koiter's general theory of initial post-buckling [34-36] is used to get an indication of the imperfection-sensitivity of these shells. Following the theory the eigenfunction corresponding to the general instability load for each shell is used in a post-buckling analysis. The initial slope is calculated. If this slope indicates the existence of equilibrium positions for loads less than the critical load these positions are unstable and the shell may be imperfection-sensitive with the severity of the sensitivity indicated by how fast the load decreases. When the slope is zero, the curvature is used as an indicator.

Koiter-type analyses of unstiffened spherical shells have been done by Thompson [42], Walker [43], Hutchinson [41], and others. Hutchinson and Amazigo [55] considered eccentrically stiffened cylindrical shells.

Throughout this chapter the deformations are assumed to be axisymmetric, only load behavior case (ii) is considered, and the Mushtari-Vlasov-Donnell approximation is made.

The Energy Functional

Following the general theory the change in total potential energy experienced by the system as the shell is displaced from the primary (uniformly contracted) state to an adjacent state is first formulated.

Strain Energy of the Shell

The geometry and sign conventions are the same as presented in Figure 1. However, since the structure is assumed to behave axisymmetrically, u_ϕ is identically zero and W and u_θ are independent of ϕ . The kinematic relations derived by Sanders [66] are again used.

The midsurface strains are given by

$$\epsilon_{\theta\theta} = \frac{1}{R} (u_{\theta,\theta} + W_1 + W_0) + \frac{1}{2R^2} W_{1,\theta}^2 \quad (33a)$$

$$\epsilon_{\phi\phi} = \frac{1}{R} (\cot \theta u_\theta + W_1 + W_0) \quad (33b)$$

where W_0 is the prebuckling deformations and W_1 and u_θ are the additional displacements.

The changes in curvature are given by

$$k_{\theta\theta} = -\frac{1}{R^2} W_{1,\theta\theta} \quad (34a)$$

$$k_{\phi\phi} = -\frac{1}{R^2} \cot \theta W_{1,\theta} \quad (34b)$$

The total strains are given by

$$\epsilon_{\theta} = \epsilon_{\theta\theta} + z k_{\theta\theta} \quad (35a)$$

$$\epsilon_{\phi} = \epsilon_{\phi\phi} + z k_{\phi\phi} \quad (35b)$$

The total stresses in the shell are

$$\sigma_{\theta}^{SH} = \frac{E}{(1-\nu^2)} [\epsilon_{\theta} + \nu \epsilon_{\phi}] \quad (36a)$$

$$\sigma_{\phi}^{SH} = \frac{E}{(1-\nu^2)} [\epsilon_{\phi} + \nu \epsilon_{\theta}] \quad (36b)$$

If the Poisson effect is neglected the stresses in the stiffeners are given by

$$\sigma_{\theta}^{ST} = \bar{E} \epsilon_{\theta} \quad (37a)$$

$$\sigma_{\phi}^{ST} = \bar{E} \epsilon_{\phi} \quad (37b)$$

The strain energy per unit area of the undeformed middle surface is given by

$$K = \frac{1}{2} \left[\int_{-h/2}^{h/2} (\sigma_{\theta}^{SH} \epsilon_{\theta} + \sigma_{\phi}^{SH} \epsilon_{\phi}) dz + \frac{1}{b_{\theta}} \int_{A_{\theta}} \sigma_{\theta}^{ST} \epsilon_{\theta} dA_{\theta} \right. \\ \left. + \frac{1}{b_{\phi}} \int_{A_{\phi}} \sigma_{\phi}^{ST} \epsilon_{\phi} dA_{\phi} \right], \quad (38)$$

or, upon substitution and integration, by

$$K = \frac{1}{2} \frac{Eh}{(1-\nu^2)} [(1+\bar{\lambda})(\epsilon_{\theta\theta}^2 + \epsilon_{\phi\phi}^2) + 2\nu\epsilon_{\theta\theta}\epsilon_{\phi\phi} + 2e\bar{\lambda}(\epsilon_{\theta\theta}k_{\theta\theta} \\ + \epsilon_{\phi\phi}k_{\phi\phi}) + e^2\bar{\lambda}(k_{\theta\theta}^2 + k_{\phi\phi}^2)] + \frac{1}{2} \frac{Eh^3}{12(1-\nu^2)} [(1+\rho)(k_{\theta\theta}^2 \\ + k_{\phi\phi}^2) + 2\nu k_{\theta\theta}k_{\phi\phi}]. \quad (39)$$

The strain energy of the shell can finally be written as

$$J_E = \frac{EhR^2}{(1-\nu^2)} \int_0^{\pi} \sin \theta \left\{ \frac{2}{R^2} W_0^2(1+\bar{\lambda}+\nu) + \frac{2}{R} W_0(1+\bar{\lambda}+\nu) \left(\frac{2}{R} W_1 \right. \right. \\ \left. \left. + \frac{1}{R} u_{\theta,\theta} + \frac{1}{R} \cot \theta u_{\theta} \right) + (1+\bar{\lambda}) \left[\left(\frac{1}{R} u_{\theta,\theta} + \frac{1}{R} W_1 \right)^2 \right. \right. \\ \left. \left. + \left(\frac{1}{R} \cot \theta u_{\theta} + \frac{1}{R} W_1 \right)^2 \right] + 2\nu \left(\frac{1}{R} u_{\theta,\theta} + \frac{1}{R} W_1 \right) \left(\frac{1}{R} \cot \theta u_{\theta} \right. \right. \\ \left. \left. + \frac{1}{R} W_1 \right) + \frac{1}{R} W_0(1+\bar{\lambda}+\nu) \left[\frac{1}{R^2} W_{1,\theta}^2 + \frac{1}{R^2} W_{1,\theta}^2 [(1+\bar{\lambda}) \frac{1}{R} u_{\theta,\theta} \right. \right. \right. \quad (40)$$

$$\begin{aligned}
& + \nu \frac{1}{R} \cot \theta u_{\theta} + (1+\bar{\lambda}+\nu) \frac{1}{R} W_1 - \bar{\lambda} \frac{e}{R} \frac{1}{R} W_{1,\theta\theta}] + \frac{1}{4}(1+\bar{\lambda}) \frac{1}{R^4} W_{1,\theta}^4 \\
& - 2\bar{\lambda} \frac{e}{R} \frac{1}{R} W_0 \left(\frac{1}{R} W_{1,\theta\theta} + \frac{1}{R} \cot \theta W_{1,\theta} \right) - 2\bar{\lambda} \frac{e}{R} \frac{1}{R} W_{1,\theta\theta} \left(\frac{1}{R} u_{\theta,\theta} \right. \\
& \left. + \frac{1}{R} W_1 \right) - 2\bar{\lambda} \frac{e}{R} \cot \theta \frac{1}{R} W_{1,\theta} \left(\frac{1}{R} \cot \theta u_{\theta} + \frac{1}{R} W_1 \right) + \bar{\lambda} \frac{e^2}{R^2} \left(\frac{1}{R^2} W_{1,\theta\theta}^2 \right. \\
& \left. + \frac{1}{R^2} \cot^2 \theta W_{1,\theta}^2 \right) + \alpha(1+\rho) \left(\frac{1}{R^2} W_{1,\theta\theta}^2 + \frac{1}{R^2} \cot^2 \theta W_{1,\theta}^2 \right) \\
& + 2\alpha\nu \frac{1}{R^2} \cot \theta W_{1,\theta} W_{1,\theta\theta} \} d\theta .
\end{aligned}$$

Potential Energy of the Load

The potential energy of the load, J_L , can be written as $(-P)$ times the change in volume, ΔV , of the shell. Now it is found convenient to shift the reference of the potential by $(-P)$ times the initial volume, V_0 , so that J_L can be written as

$$J_L = -PV. \quad (41)$$

With the aid of Sylvester's paper [67] the deformed volume, V , of the shell can be expressed as

$$V = \pi R^3 \int_0^\pi \sin^3 \theta \left[(1+\epsilon_{\phi\phi})^3 + (1+\epsilon_{\phi\phi})^2 \left(\frac{1}{R} u_{\theta,\theta} - \frac{1}{R} \cot \theta W_{1,\theta} \right) \right] d\theta \quad (42)$$

The potential of the load can then be written as

$$J_L = \frac{EhR^2}{(1-\nu^2)} \int_0^\pi -2\bar{\beta} \sin^3 \theta \left\{ \left(1 + \frac{1}{R} W_0\right)^3 + \left(1 + \frac{1}{R} W_0\right)^2 \left[3\left(\frac{1}{R} \cot \theta \cdot \right. \right. \right. (43)$$

$$\left. \left. u_\theta + \frac{1}{R} W_1\right) + \left(\frac{1}{R} u_{\theta,\theta} - \frac{1}{R} \cot \theta W_{1,\theta}\right) \right] + \left(1 + \frac{1}{R} W_0\right) \cdot \right.$$

$$\left. \left[3\left(\frac{1}{R} \cot \theta u_\theta + \frac{1}{R} W_1\right)^2 + 2\left(\frac{1}{R} u_{\theta,\theta} - \frac{1}{R} \cot \theta W_{1,\theta}\right) \cdot \right. \right.$$

$$\left. \left(\frac{1}{R} \cot \theta u_\theta + \frac{1}{R} W_1\right) \right] + \left[\left(\frac{1}{R} \cot \theta u_\theta + \frac{1}{R} W_1\right)^3 + \left(\frac{1}{R} u_{\theta,\theta} \right. \right.$$

$$\left. \left. - \frac{1}{R} \cot \theta W_{1,\theta}\right) \left(\frac{1}{R} \cot \theta u_\theta + \frac{1}{R} W_1\right)^2 \right] \} d\theta$$

where the load parameter, $\bar{\beta}$, is given by

$$\bar{\beta} = PR(1-\nu^2)/2Eh \quad (44)$$

The First Expansion of the Energy Functional

The energy functional, $P[u_\theta, W_1]$, is the sum of the potential energy of the shell and that of the load. According to the general theory it is first expanded in the form

$$P[u_\theta, W_1] = P_0 + P_1[u_\theta, W_1] + P_2[u_\theta, W_1] + \dots \quad (45)$$

where $P_m[u_\theta, W_1]$ is the sum of all terms of m th degree in the buckling displacements and their derivatives. This expansion ends with

$P_4[u_\theta, W_1]$ in the present case since this is the highest order term in the expressions for J_E and J_L .

These terms are as follows:

$$P_0 = \frac{\pi E h R^2}{(1-\nu^2)} \left[4(1+\bar{\lambda}+\nu) \frac{1}{R^2} W_0^2 - \frac{8}{3} \bar{\beta} \left(1 + \frac{1}{R} W_0 \right)^3 \right] \quad (46a)$$

$$P_1[u_\theta, W_1] = \frac{\pi E h R^2}{(1-\nu^2)} \int_0^\pi \sin \theta \left\{ \frac{2}{R} W_0 (1+\bar{\lambda}+\nu) \left[\frac{2}{R} W_1 + \frac{1}{R} u_{\theta,\theta} \right. \right. \quad (46b)$$

$$\begin{aligned} &+ \frac{1}{R} \cot \theta u_\theta \left. - 2\bar{\beta} \left(1 + \frac{1}{R} W_0 \right)^2 \sin^2 \theta \left[3 \left(\frac{1}{R} \cot \theta u_\theta \right. \right. \right. \\ &+ \frac{1}{R} W_1 \left. \right) + \left(\frac{1}{R} u_{\theta,\theta} - \frac{1}{R} \cot \theta W_{1,\theta} \right) \left. - 2\bar{\lambda} \frac{e}{R} \frac{1}{R} W_0 \left(\frac{1}{R} W_{1,\theta\theta} \right. \right. \\ &\left. \left. + \frac{1}{R} \cot \theta W_{1,\theta} \right) \right\} d\theta \end{aligned}$$

$$P_2[u_\theta, W_1] = \frac{\pi E h R^2}{(1-\nu^2)} \int_0^\pi \sin \theta \left\{ (1+\bar{\lambda}) \left[\left(\frac{1}{R} u_{\theta,\theta} + \frac{1}{R} W_1 \right)^2 \right. \right. \quad (46c)$$

$$\begin{aligned} &+ \left(\frac{1}{R} \cot \theta u_\theta + \frac{1}{R} W_1 \right)^2 \left. \right] + 2\nu \left(\frac{1}{R} u_{\theta,\theta} + \frac{1}{R} W_1 \right) \left(\frac{1}{R} \cot \theta u_\theta \right. \\ &+ \frac{1}{R} W_1 \left. \right) + \frac{1}{R} W_0 (1+\bar{\lambda}+\nu) \frac{1}{R^2} W_{1,\theta}^2 + \left[\alpha(1+\rho) + \bar{\lambda} \frac{e^2}{R^2} \right] \cdot \end{aligned}$$

$$\left[\frac{1}{R^2} W_{1,\theta\theta}^2 + \frac{1}{R^2} \cot^2 \theta W_{1,\theta}^2 \right] + 2\alpha\nu \frac{1}{R^2} \cot \theta W_{1,\theta} W_{1,\theta\theta}$$

$$- 2\bar{\beta} \left(1 + \frac{1}{R} W_0 \right) \sin^2 \theta \left[3 \left(\frac{1}{R} \cot \theta u_\theta + \frac{1}{R} W_1 \right)^2 \right.$$

$$\left. + 2 \left(\frac{1}{R} \cot \theta u_\theta + \frac{1}{R} W_1 \right) \left(\frac{1}{R} u_{\theta,\theta} - \frac{1}{R} \cot \theta W_{1,\theta} \right) \right]$$

$$- 2\bar{\lambda} \frac{e}{R} \frac{1}{R} W_{1,\theta\theta} \left(\frac{1}{R} u_{\theta,\theta} + \frac{1}{R} W_1 \right) - 2\bar{\lambda} \frac{e}{R} \cot \theta \frac{1}{R} W_{1,\theta} \left(\frac{1}{R} \cot \theta u_{\theta} + \frac{1}{R} W_1 \right) \} d\theta$$

$$\begin{aligned} P_3[u_{\theta}, W_1] = & \frac{\pi E h R^2}{(1-\nu^2)} \int_0^{\pi} \sin \theta \left\{ \frac{1}{2} W_{1,\theta}^2 \left[(1+\bar{\lambda}) \frac{1}{R} u_{\theta,\theta} \right. \right. \\ & + \nu \frac{1}{R} \cot \theta u_{\theta} + \frac{1}{R} W_1 (1+\bar{\lambda}+\nu) - \bar{\lambda} \frac{e}{R} \frac{1}{R} W_{1,\theta\theta}] \\ & - 2\bar{\beta} \sin^2 \theta \left[\left(\frac{1}{R} \cot \theta u_{\theta} + \frac{1}{R} W_1 \right)^3 + \left(\frac{1}{R} \cot \theta u_{\theta} \right. \right. \\ & \left. \left. + \frac{1}{R} W_1 \right)^2 \left(\frac{1}{R} u_{\theta,\theta} - \frac{1}{R} \cot \theta W_{1,\theta} \right) \right] \} d\theta \end{aligned} \quad (46d)$$

$$P_4[u_{\theta}, W_1] = \frac{\pi E h R^2}{(1-\nu^2)} \int_0^{\pi} \frac{1}{4} (1+\bar{\lambda}) \sin \theta \frac{1}{R^4} W_{1,\theta}^4 d\theta \quad (46e)$$

Primary State

The principle of the minimum value of the total potential requires that the first variation of the energy functional with respect to the displacements be zero for all positions of equilibrium. The primary state is a position of equilibrium for which this variation reduces to the variation of $P_1[u_{\theta}, W_1]$. Thus the variation of $P_1[u_{\theta}, W_1]$ must be identically zero. This requirement leads to the following relation between the prebuckling deflection and the load parameter:

$$(1+\bar{\lambda}+\nu) \frac{1}{R} W_0 = \bar{\beta} \left(1 + \frac{1}{R} W_0 \right)^2. \quad (47)$$

For small values of $\bar{\beta}$ and $\frac{1}{R} W_0$ this reduces to the relation

$$\frac{1}{R} W_0 = \bar{\beta}/(1+\bar{\lambda}+\nu), \quad (48)$$

which agrees with the primary state solution.

The introduction of Equation (48) into Equation (46c) and neglect of $\frac{1}{R} W_0$ in direct comparison with unity gives the following functional to be used in the eigenvalue analysis:

$$\begin{aligned} P_2[u_\theta, W_1] = & \frac{\pi E h R^2}{(1-\nu^2)} \int_0^\pi \sin \theta \{ (1+\bar{\lambda}) \left[\left(\frac{1}{R} u_{\theta,\theta} + \frac{1}{R} W_1 \right)^2 \right. \\ & + \left. \left(\frac{1}{R} \cot \theta u_\theta + \frac{1}{R} W_1 \right)^2 \right] + 2\nu \left(\frac{1}{R} u_{\theta,\theta} + \frac{1}{R} W_1 \right) \cdot \\ & \left(\frac{1}{R} \cot \theta u_\theta + \frac{1}{R} W_1 \right) + \bar{\beta} \frac{1}{R^2} W_{1,\theta}^2 + [\alpha(1+\rho) \\ & + \bar{\lambda} \frac{e^2}{R^2}] \left[\frac{1}{R^2} W_{1,\theta\theta}^2 + \frac{1}{R^2} \cot^2 \theta W_{1,\theta}^2 \right] + 2\alpha\nu \frac{1}{R^2} \cdot \\ & \cot \theta W_{1,\theta} W_{1,\theta\theta} - 2\bar{\beta} \sin^2 \theta \left[3 \left(\frac{1}{R} \cot \theta u_\theta \right. \right. \\ & + \left. \left. \frac{1}{R} W_1 \right)^2 + 2 \left(\frac{1}{R} \cot \theta u_\theta + \frac{1}{R} W_1 \right) \left(\frac{1}{R} u_{\theta,\theta} \right. \right. \\ & - \left. \left. \frac{1}{R} \cot \theta W_{1,\theta} \right) \right] - 2\bar{\lambda} \frac{e}{R} \frac{1}{R} W_{1,\theta\theta} \left(\frac{1}{R} u_{\theta,\theta} + \frac{1}{R} W_1 \right) \\ & - 2\bar{\lambda} \frac{e}{R} \cot \theta \frac{1}{R} W_{1,\theta} \left(\frac{1}{R} \cot \theta u_\theta + \frac{1}{R} W_1 \right) \} d\theta. \end{aligned} \quad (49)$$

The Second Expansion of the Energy Functional

Still following the general theory each component of $P[u_\theta, W_1]$ is expanded as a power series in $(\bar{\beta} - \bar{\beta}_{CR})$, where $\bar{\beta}_{CR}$ is the, as yet undetermined, critical value of $\bar{\beta}$, as follows:

$$P_m[u_\theta, W_1] = P_m^0[u_\theta, W_1] + (\bar{\beta} - \bar{\beta}_{CR})P_m^1[\] + \dots \quad (50)$$

The term necessary for the post-buckling analysis are given by

$$P_2^1[u_\theta, W_1] = \frac{\pi E h}{(1-\nu^2)} \int_0^\pi \{ \sin \theta W_{1,\theta}^2 - 2 \sin^3 \theta [3(\cot \theta u_\theta + W_1)^2 + 2(\cot \theta u_\theta + W_1)(u_{\theta,\theta} - \cot \theta W_{1,\theta})] \} d\theta \quad (51a)$$

$$P_3^0[u, W_1] = \frac{\pi E h}{R(1-\nu^2)} \int_0^\pi \{ \sin \theta W_{1,\theta}^2 [(1+\bar{\lambda})u_{\theta,\theta} + \nu \cot \theta u_\theta + (1+\bar{\lambda}+\nu)W_1 - \bar{\lambda} \frac{e}{R} W_{1,\theta\theta}] - 2\bar{\beta}_{CR} \sin^3 \theta [(\cot \theta u_\theta + W_1)^3 + (\cot \theta u_\theta + W_1)^2 (u_{\theta,\theta} - \cot \theta W_{1,\theta})] \} d\theta \quad (51b)$$

$$P_4^0[u_\theta, W_1] = \frac{\pi E h}{4R^2(1-\nu^2)} (1+\bar{\lambda}) \int_0^\pi \sin \theta W_{1,\theta}^4 d\theta. \quad (51c)$$

Eigenvalue Analysis

The linear eigenvalue problem corresponding to the strain energy functional derived in the previous section can now be solved to obtain

the eigenvalues (general instability loads) and the corresponding eigenfunctions which are required for the initial post-buckling analysis.

Stability Equations

The principle of the minimum value of the total potential is again applied to obtain the stability equations. This principle, as stated earlier, requires that the first variation of the energy functional with respect to the displacements be identically zero for equilibrium. In the linear analysis the increments are assumed so small that $P_3[u_\theta, W_1]$ and $P_4[u_\theta, W_1]$ can be neglected. P_0 is a constant and its variation is identically zero. The variation of $P_1[u_\theta, W_1]$ was required to be zero to insure that the primary state is a position of equilibrium. The principle thus requires that the first variation of $P_2[u_\theta, W_1]$ with respect to the increments be zero for the existence of adjacent equilibrium.

From these requirements the following two stability equations are obtained:

$$[(1+\bar{\lambda})\left(\frac{\partial^2}{\partial \theta^2} + \cot \theta \frac{\partial}{\partial \theta} - \cot^2 \theta\right) + 2\beta - \nu] u_\theta + [-\bar{\lambda} \frac{e}{R} \left(\frac{\partial^3}{\partial \theta^3}\right. \quad (52a)$$

$$\left. + \cot \theta \frac{\partial^2}{\partial \theta^2} - \cot^2 \theta \frac{\partial}{\partial \theta}\right) + (1+\bar{\lambda} + \nu - 2\beta) \frac{\partial}{\partial \theta}] W_1 = 0$$

$$\{-\bar{\lambda} \frac{e}{R} \left(\frac{\partial^3}{\partial \theta^3} + 2\cot \theta \frac{\partial^2}{\partial \theta^2} - \cot^2 \theta \frac{\partial}{\partial \theta} - 2 \frac{\partial}{\partial \theta} + \csc^2 \theta \cot \theta\right) \quad (52b)$$

$$+ (1+\bar{\lambda} + \nu - \bar{\lambda} \frac{e}{R} - 2\beta) \left(\frac{\partial}{\partial \theta} + \cot \theta\right) u_\theta + \{[\alpha(1+\rho) + \bar{\lambda} \frac{e^2}{R^2}]\}$$

$$\begin{aligned}
& \left(\frac{\partial^4}{\partial \theta^4} + 2 \cot \theta \frac{\partial^3}{\partial \theta^3} - \cot^2 \theta \frac{\partial^2}{\partial \theta^2} - 2 \frac{\partial^2}{\partial \theta^2} + \csc^2 \theta \cot \theta \frac{\partial}{\partial \theta} \right) \\
& + [\alpha(1+\rho) + \bar{\lambda} \frac{e^2}{R^2} - 2\bar{\lambda} \frac{e}{R} - \alpha v - \beta] \left(\frac{\partial^2}{\partial \theta^2} + \cot \theta \frac{\partial}{\partial \theta} \right) \\
& + 2(1+\bar{\lambda}+v-2\beta) W_1 = 0.
\end{aligned}$$

Reduction of the Equations

The stability equations, Equations (52), can be reduced to a more convenient form by the introduction of a displacement potential, \bar{S} , such that

$$\bar{S}_{,\theta} = u_\theta, \quad (53)$$

and by defining a linear differential operator, $\bar{\nabla}^2$, such that

$$\bar{\nabla}^2 = \frac{\partial^2}{\partial \theta^2} + \cot \theta \frac{\partial}{\partial \theta}. \quad (54)$$

This form is as follows:

$$\frac{\partial}{\partial \theta} \{ [(1+\bar{\lambda})\bar{\nabla}^2 + 1 + \bar{\lambda} - v + 2\beta] \bar{S} + [-\bar{\lambda} \frac{e}{R} \bar{\nabla}^2 \quad (55a)$$

$$+ 1 + \bar{\lambda} + v - \bar{\lambda} \frac{e}{R} - 2\beta] W_1 \} = 0$$

$$\{ \bar{\nabla}^2 [-\bar{\lambda} \frac{e}{R} \bar{\nabla}^2 + 1 + \bar{\lambda} + v - \bar{\lambda} \frac{e}{R} - 2\beta] \bar{S} + \{ [\alpha(1+\rho) \quad (55b)$$

$$+ \bar{\lambda} \frac{e^2}{R^2} \bar{\nabla}^4 + [\alpha(1+\rho) + \bar{\lambda} \frac{e^2}{R^2} - 2\bar{\lambda} \frac{e}{R} - \alpha v - \beta] \bar{\nabla}^2$$

$$+ 2(1 + \bar{\lambda} + \nu - 2\beta))W_1 = 0$$

Next Equation (55a) is integrated with respect to θ , the constant of integration is set equal to zero (as was done in Chapter II), and β is neglected in direct comparison with unity. The stability equations then take the form

$$\{(1+\bar{\lambda})\bar{\nu}^2+1+\bar{\lambda}-\nu\}\bar{S} + \{-\bar{\lambda} \frac{e}{R} \bar{\nu}^2+1+\bar{\lambda}+\nu-\bar{\lambda} \frac{e}{R}\}W_1 = 0 \quad (56a)$$

$$\{\bar{\nu}^2[-\bar{\lambda} \frac{e}{R} \bar{\nu}^2+1+\bar{\lambda}+\nu-\bar{\lambda} \frac{e}{R}]\}\bar{S} + \{[\alpha(1+\rho) + \bar{\lambda} \frac{e^2}{R^2}]\bar{\nu}^4 \quad (56b)$$

$$+ [\alpha(1+\rho-\nu) + \bar{\lambda} \frac{e^2}{R^2} - 2\bar{\lambda} \frac{e}{R} - \beta]\bar{\nu}^2 + 2(1+\bar{\lambda}+\nu)\}W_1 = 0.$$

Solution of the Stability Equations

The eigenfunctions of the stability equations, Equations (56), are Legendre polynomials. The additional increments are thus assumed in the form

$$W_1(\theta) = \sum_{n=0}^{\infty} a_n P_n(\cos \theta) \quad (57a)$$

$$\bar{S}(\theta) = \sum_{n=0}^{\infty} b_n P_n(\cos \theta) \quad (57b)$$

where a_n and b_n are undetermined coefficients.

Substitution of Equations (57) into the Equations (56) gives the two algebraic equations,

$$\{-(1+\bar{\lambda})n(n+1)+1+\bar{\lambda}-v\}b_n + \{\bar{\lambda} \frac{e}{R} n(n+1)+1+\bar{\lambda}+v-\bar{\lambda} \frac{e}{R}\}a_n = 0 \quad (58a)$$

$$\{-n(n+1)[\bar{\lambda} \frac{e}{R} n(n+1)+1+\bar{\lambda}+v-\bar{\lambda} \frac{e}{R}]\}b_n + \{[\alpha(1+\rho)+\bar{\lambda} \frac{e^2}{R^2}]n^2(n+1)^2 \quad (58b)$$

$$+ [-\alpha(1+\rho-v)-\bar{\lambda} \frac{e^2}{R^2} + 2\bar{\lambda} \frac{e}{R} + \beta]n(n+1) + 2(1+\bar{\lambda}+v)\}a_n = 0$$

which must be satisfied for each n .

In order to satisfy Equations (58) take

$$b_n = \{[\bar{\lambda} \frac{e}{R} n(n+1)+1+\bar{\lambda}+v-\bar{\lambda} \frac{e}{R}]/[(1+\bar{\lambda})n(n+1)-1-\bar{\lambda}+v]\}a_n, \quad (59)$$

and

$$P_{CR}/P_{CL} = [\frac{1}{3}(1-v^2)]^{-1/2} \frac{R}{h} \{-[\bar{\lambda} \frac{e}{R} n(n+1)+1+\bar{\lambda}+v-\bar{\lambda} \frac{e}{R}]^2/[(1+\bar{\lambda})n(n+1) \quad (60)$$

$$- 1-\bar{\lambda}+v] + [\alpha(1+\rho)+\bar{\lambda} \frac{e^2}{R^2}]n(n+1) - \alpha(1+\rho-v) - \bar{\lambda} \frac{e^2}{R^2}$$

$$+ 2\bar{\lambda} \frac{e}{R} + 2(1+\bar{\lambda}+v)/n(n+1)\},$$

where $P_{CL} = -2E(\frac{h}{R})^2/\sqrt{3(1-v^2)}$.

The non-dimensional general instability loads, $(P_{CR}/P_{CL})_{MIN.}$, are determined by the minimization of Equation (60) with respect to integer values of n . The value of n which corresponds to $(P_{CR}/P_{CL})_{MIN.}$ is denoted by n_{CR} .

The increments which are to be used in the initial post-buckling analysis are given by the relations

$$W_{l_{CR}} = a_{n_{CR}} P_{n_{CR}} (\cos \theta) \quad (61a)$$

$$u_{CR} = B a_{n_{CR}} P_{n_{CR}} (\cos \theta), \quad (61b)$$

where

$$B = [\bar{\lambda} \frac{e}{R} n_{CR}(n_{CR}+1)+1+\bar{\lambda}+\nu-\bar{\lambda} \frac{e}{R}] / [(1+\bar{\lambda})n_{CR}(n_{CR}+1)-1-\bar{\lambda}+\nu]. \quad (62)$$

Imperfection-Sensitivity Study

With the linear eigenvalue problem solved, attention is turned to the initial post-buckling behavior of the shells to obtain an indication of their imperfection-sensitivity. This attention is focused on the first branching point.

General Procedure

According to the general theory the linear eigenfunctions (the increments corresponding to the general instability loads) and the eigenvalues (written as β_{CR}) are substituted into the energy functional. This substitution gives the following:

$$P \left[\frac{u_{\theta_{CR}}}{a_{n_{CR}}}, \frac{W_{l_{CR}}}{a_{n_{CR}}} \right] = P_0^0 + a_{n_{CR}} P_1^0 \left[\frac{u_{\theta_{CR}}}{a_{n_{CR}}}, \frac{W_{l_{CR}}}{a_{n_{CR}}} \right] \quad (63)$$

$$\begin{aligned}
& + a_{n_{CR}}^2 P_2^0[] + a_{n_{CR}}^3 P_3^0[] + a_{n_{CR}}^4 P_4^0[] \\
& + (\bar{\beta} - \bar{\beta}_{CR}) \{ P_0^1 + a_{n_{CR}} P_1^1[] + a_{n_{CR}}^2 P_2^1[] + a_{n_{CR}}^3 P_3^1[] \}.
\end{aligned}$$

As can be seen from Equation (63) the initial post-buckling problem is thus reduced to the study of a system which has only one degree of freedom (namely $a_{n_{CR}}$). To determine the post-buckling equilibrium positions of this system the derivative of Equation (63) with respect to $a_{n_{CR}}$ is set to zero. The post-buckling equilibrium positions are thus given by the following:

$$\begin{aligned}
dP[]/da_{n_{CR}} &= P_1^0[] + 2a_{n_{CR}} P_2^0[] + 3a_{n_{CR}}^2 P_3^0[] \\
&+ 4a_{n_{CR}}^3 P_4^0[] + (\bar{\beta} - \bar{\beta}_{CR}) \{ P_1^1[] + 2a_{n_{CR}} P_2^1[] \\
&+ 3a_{n_{CR}}^2 P_3^1[] \} = 0.
\end{aligned} \tag{64}$$

Since the primary state given by $a_{n_{CR}} = 0$ must be a position of equilibrium, it follows that

$$P_1^0[] + (\bar{\beta} - \bar{\beta}_{CR}) P_1^1[] = 0. \tag{65}$$

Since $P_2 \left[\frac{u_{\theta_{CR}}}{a_{n_{CR}}}, \frac{w_{1_{CR}}}{a_{n_{CR}}} \right]$ is equal to zero at the bifurcation point, it follows that

$$P_2^0 \left[\frac{u_{\theta CR}}{a_{nCR}}, \frac{w_{1CR}}{a_{nCR}} \right] = 0 \quad (66)$$

Substitution of Equations (65) and (66) into Equation (64) gives the following condition from which the post-buckling equilibrium positions can be obtained:

$$a_{nCR} (3a_{nCR} P_3^0[\] + 4a_{nCR}^2 P_4^0[\] + (\bar{\beta} - \bar{\beta}_{CR}) \{ 2P_2^1[\] + 3a_{nCR} P_3^1[\] \}) = 0. \quad (67)$$

From Equation (67) it is seen that post-buckling equilibrium positions exist if either $a_{nCR} = 0$, which is a trivial solution, or

$$P/P_{CR_{MIN}} = 1 - \{ 3 \left(\frac{a_{nCR}}{h} \right) P_3^0[\] h + 4 \left(\frac{a_{nCR}}{h} \right)^2 P_4^0[\] h^2 \} / \bar{\beta}_{CR} \{ 2P_2^1[\] + 3 \left(\frac{a_{nCR}}{h} \right) P_3^1[\] h \}. \quad (68)$$

The initial post-buckling slope is obtained from Equation (68) as follows:

$$d(P/P_{CR_{MIN}})/d(a_{nCR}/h) \Big|_{a_{nCR}=0} = - \frac{3P_3^0[\] h}{2\bar{\beta}_{CR} P_2^1[\]} \quad (69)$$

The initial post-buckling slope given by Equation (69) is zero

when $P_3^0[\] = 0$. An upper bound to the post-buckling curvature is given by the relation which follows:

$$d^2(P/P_{CR_{MIN}})/d(a_{n_{CR}}/h)^2 \Big|_{a_{n_{CR}}=0} = - \frac{4P_4^0[\]h}{\bar{\beta}_{CR} P_2^1[\]} \quad (70)$$

This is an approximation that does not fully account for the redistribution of stress for finite $a_{n_{CR}}$. A rigorous result could be obtained, in general, by the method outlined in [35-37]. In view of the limited usefulness of Koiter-theory results, the additional analysis required to obtain a rigorous curvature measure does not seem justified.

Evaluation of the Required Functionals

Substitution of the eigenfunctions, Equations (61), into the required functionals, Equations (51), integration by parts, and a change in variables as demonstrated in Appendix C reduce these functionals to the following form:

$$P_2^1 \left[\frac{u_{\theta_{CR}}}{a_{n_{CR}}}, \frac{w_{l_{CR}}}{a_{n_{CR}}} \right] = \frac{\pi E h}{(1-\nu^2)} \{ [-2B^2 + 4B + 1] n_{CR}(n_{CR} + 1) \quad (71)$$

$$- 4 \} \int_{-1}^1 [P_{n_{CR}}(x)]^2 dx$$

$$P_3^0 \left[\frac{u_{\theta_{CR}}}{a_{n_{CR}}}, \frac{w_{l_{CR}}}{a_{n_{CR}}} \right] = \frac{\pi E h}{R(1-\nu^2)} \{ [B^3 \bar{\beta}_{CR} - \frac{3}{2} B^2 \beta_{CR} + \frac{1}{4} B(1+\bar{\lambda}-3\nu) \quad (72)$$

$$\begin{aligned}
& - \frac{1}{4} \bar{\lambda} \frac{e}{R} n_{CR}^2 (n_{CR}+1)^2 + [-B^2 \bar{\beta}_{CR} + 2B \bar{\beta}_{CR} + \frac{1}{2}(1+\bar{\lambda}+\nu)] n_{CR} (n_{CR}+1) \\
& - \frac{4}{3} \bar{\beta}_{CR} \int_{-1}^1 [P_{n_{CR}}(x)]^3 dx \\
P_4^0 \left[\frac{u_{\theta CR}}{a_{n_{CR}}}, \frac{w_{l CR}}{a_{n_{CR}}} \right] &= \frac{\pi E h}{4R^2(1-\nu^2)} (1+\bar{\lambda}) \int_{-1}^1 [P_{n_{CR}}(x)]^4 dx; \text{ ODD } n_{CR} \quad (73)
\end{aligned}$$

Lebedev [68] shows that

$$\int_{-1}^1 [P_n(x)]^2 dx = 2/(2n+1). \quad (74)$$

Thompson [42] shows that

$$\int_{-1}^1 [P_n(x)]^3 dx = \begin{cases} \frac{4\sqrt{3}}{3\pi} \frac{1}{n(n+1)} & ; \text{ even } n \\ 0 & ; \text{ odd } n \end{cases} \quad (75)$$

Walker [43] shows that

$$[P_n(x)]^2 = \sum_{i=0}^n \frac{[A(n-i)]^2 A(i)[4n-4i+1]}{A(2n-i)[4n-2i+1]} P_{2(n-i)}(x) \quad (76)$$

where

$$A(m) = \frac{1 \cdot 3 \cdot 5 \cdot \dots \cdot (2m-1)}{1 \cdot 2 \cdot 3 \cdot \dots \cdot m} \quad (77a)$$

$$A(0) = A(-m) = 0 \quad (77b)$$

Using Equation (76) and orthogonality it can be shown that

$$\int_{-1}^1 [P_n(x)]^4 dx = \sum_{i=0}^n \frac{2[A(n-i)]^4 [A(i)]^2 (4n-4i+1)^2}{[A(2n-i)]^2 (4n-2i+1)^2 [4(n-i)+1]} \quad (78)$$

The required functionals can then be written as

$$P_2^1[\] = \frac{\pi E h}{(1-v^2)} C_{n_{CR}} \quad (79)$$

$$P_3^0[\] = \frac{E h}{R(1-v^2)} D_{n_{CR}} \quad (80)$$

$$P_4^0[\] = \frac{\pi E h}{R^2(1-v^2)} (1+\bar{\lambda}) E_{n_{CR}} \quad (81)$$

where

$$C_{n_{CR}} = \frac{2}{2n_{CR} + 1} \{ [-2B^2 + 4B + 1] n_{CR} (n_{CR} + 1) - 4 \} \quad (82a)$$

$$D_{n_{CR}} = \begin{cases} \frac{4\sqrt{3}}{3} \left\{ -\sqrt{\frac{1}{3}} (1-\nu^2) \left(\frac{h}{R}\right) (P_{CR}/P_{CL})_{MIN} [B^2(B - \frac{3}{2}) n_{CR}(n_{CR}+1) \right. \\ + B(-B+2) - \frac{4}{3n_{CR}(n_{CR}+1)}] + \frac{1}{4} [B(1+\bar{\lambda}-3\nu) - \bar{\lambda} \frac{e}{R}] n_{CR}(n_{CR}+1) \\ \left. + \frac{1}{2}(1+\bar{\lambda}+\nu) \right\} ; & \text{even } n_{CR} \\ 0 & ; \quad \text{odd } n_{CR} \end{cases} \quad (82b)$$

$$E_{n_{CR}} = \sum_{i=0}^{n_{CR}} \frac{[A(n_{CR}-i)]^4 [A(i)]^2 [4(n_{CR}-i)+1]^2}{[A(2n_{CR}-i)]^2 [4n_{CR}-2i+1]^2 [8(n_{CR}-i)+2]} ; \text{ odd } n_{CR} \quad (82c)$$

Completion of the Study

Substitution of Equations (79) and (80) into Equation (69) gives the initial post-buckling slope as shown below

$$d(P/P_{CR_{MIN}})/d(a_{n_{CR}}/h) \Big|_{a_{n_{CR}=0}} = \frac{3\sqrt{3} D_{n_{CR}}}{2\pi\sqrt{(1-\nu^2)} (P_{CR}/P_{CL})_{MIN} C_{n_{CR}}} \quad (83)$$

For odd values of n_{CR} the initial post-buckling slope is zero and the initial post-buckling curvature is given as

$$d^2(P/P_{CR_{MIN}})/d(a_{n_{CR}}/h)^2 \Big|_{a_{n_{CR}=0}} = \frac{4\sqrt{3} (h/R)(1+\bar{\lambda}) E_{n_{CR}}}{\sqrt{(1-\nu^2)} (P_{CR}/P_{CL})_{MIN} C_{n_{CR}}} \quad (84)$$

With the use of Equations (83) and (84) an indication of the imperfection-sensitivity of these shells can be obtained.

Discussion and Conclusions

A numerical study of Equation (83) was made to determine the initial post-buckling slopes for some typical shells. For making this study, a computer program was written for the Univac 1108. This program is contained in Appendix D. Throughout the numerical work the value $\nu = 1/3$ was used. Table 2 contains some sample results from this program.

From Table 2 it can be observed that the suggested initial post-buckling slopes are small and positive when n_{CR} is even and zero when n_{CR} is odd. When the slope is zero Equation (84) suggests that the curvature is positive (since $E_{n_{CR}}$ and $C_{n_{CR}}$ are positive). Thus the analysis suggests that shells which correspond to even values of n_{CR} are imperfection-sensitive and those which correspond to odd values are not. This suggested initial post-buckling behavior is illustrated in Figure 7. The dotted positions are unstable.

The results of an analysis of unstiffened spherical shells by Thompson [42] indicated this same type of behavior. However, Thompson rejected the suggested imperfection-insensitivity with the explanation that the bifurcation points are so closely spaced that the modes corresponding to the odd values of n_{CR} will never be seen.

This explanation was based on the observation that structures which have closely spaced bifurcation points often follow a post-buckling path which is different from that suggested by n_{CR} . From a

practical point of view this path could correspond to a discrete mode with a different mode number (say $n_{CR}-1$), it could involve a change in mode as discussed by Stein [69], or it could even involve a coupling of modes as mentioned by Chilver [70]. From this observation it would seem that any single mode analysis as used by Thompson [42] and as used in this thesis should be accompanied by a study of the spacing of the bifurcation points and in some cases a multimode analysis may be appropriate. Such a study was made here. Some typical results are shown in Figure 8.

From these results (Table 2 and Figure 8) the following major conclusions may be drawn:

1. The meaning of this analysis is questionable for lightly stiffened shells which have closely spaced bifurcation points as shown in Figure 8a. (In cases like this, modal "coupling" is likely to occur and a multimode study is desirable).

2. For moderately or heavily stiffened shells which have sufficiently spaced bifurcation points as shown in Figures 8b, c, and d, the following statements can be made: (i) the results obtained for even values of n_{CR} can be used as the indicator for imperfection-sensitivity (the odd value of n_{CR} will not be seen because of the proximity of the loads corresponding to even values of n as shown in Figure 8b); (ii) the degree of imperfection-sensitivity is directly proportional to $\bar{\lambda}$ and inversely proportional to $|e/h|$ and ρ ; and (iii) the imperfection-sensitivity is greater for inside stiffeners than for outside stiffeners for the range of parameters studied.

Table 1. Sample Results from Both Programs

$$h/R = .002 \quad \bar{\lambda} = 0.222 \quad \rho = 5.00$$

MAKING THE MUSHTARI-VLASOV-DONNELL APPROXIMATION

FH	1	N1	2	SPR1	3	N2	SPR2	N3	SPR3	PWS1	⁴	PWS2	PWS3
-14	9	26.50	9	26.00	9	26.50	71.20	70.90	71.1				
-12	10	22.80	10	22.50	10	22.80	68.90	68.60	68.9				
-8	12	15.40	12	15.20	12	15.40	61.90	61.70	61.9				
-4	17	8.11	16	8.06	17	8.11	47.50	47.30	47.5				
0	27	2.76	27	2.75	27	2.76	9.80	9.65	9.77				
^{1/2}	17	6.35	16	6.27	17	6.35	40.30	40.00	40.30				
8	12	11.90	12	11.60	12	11.90	56.30	55.80	56.30				
12	10	17.60	10	17.10	10	17.60	64.00	63.40	64.00				
14	9	20.50	9	19.70	9	20.50	66.60	65.90	66.60				

WITHOUT MAKING THE MUSHTARI-VLASOV-DONNELL APPROXIMATION

EH	N1	SPR1	N2	SPR2	N3	SPR3	PWS1	PWS2	PWS3
-14	9	26.20	9	25.70	9	26.20	71.00	70.70	71.00
-12	10	22.60	9	22.20	10	22.60	68.70	68.40	68.70
-8	12	15.30	12	15.10	12	15.30	61.80	61.60	61.80
-4	16	8.08	16	8.02	16	8.07	47.40	47.20	47.40
0	27	2.76	27	2.75	27	2.76	9.73	9.54	9.70
4	16	6.33	16	6.25	16	6.32	40.20	39.80	40.20
8	12	11.80	12	11.60	12	11.80	56.10	55.60	56.10
12	10	17.50	10	17.00	10	17.50	63.90	63.30	63.90
14	9	20.30	9	19.60	9	20.30	66.40	65.80	66.40

¹EH is the non-dimensional eccentricity (e/h).

² N_j is the critical mode number for load behavior case j .

³SPR _{j} is the non-dimensional general instability load for load behavior case j .

⁴PWS _{j} is the percent weight savings for load behavior case j .

Table 2. Initial Post-Buckling Slopes

e/h	(h/R = .002)					
	$\bar{\lambda}=.222$	$\rho=5$	$\bar{\lambda}=1.333$	$\rho=300$	$\bar{\lambda}=2.667$	$\rho=2000$
	n_{CR}	Slope	n_{CR}	Slope	n_{CR}	Slope
-15	9	.0000	7	.0000	7	.0000
-14	9	.0000	7	.0000	7	.0000
-13	9	.0000	8	.0072	7	.0000
-12	10	.0083	8	.0076	7	.0000
-11	10	.0090	8	.0080	7	.0000
-10	11	.0000	9	.0000	7	.0000
-9	11	.0000	9	.0000	7	.0000
-8	12	.0103	9	.0000	8	.0068
-7	13	.0000	10	.0086	8	.0069
-6	14	.0116	10	.0091	8	.0070
-5	15	.0000	10	.0097	8	.0072
-4	16	.0144	11	.0000	8	.0072
-3	19	.0000	11	.0000	8	.0073
0	27	.0000	12	.0100	8	.0073
3	19	.0000	11	.0000	8	.0071
4	16	.0145	11	.0000	8	.0069
5	15	.0000	10	.0094	8	.0067
6	14	.0113	10	.0087	8	.0065
7	13	.0000	10	.0079	8	.0063
8	12	.0100	9	.0000	8	.0061
9	11	.0000	9	.0000	7	.0000
10	11	.0000	9	.0000	7	.0000
11	10	.0088	8	.0074	7	.0000
12	10	.0079	8	.0069	7	.0000
13	9	.0000	8	.0063	7	.0000
14	9	.0000	8	.0058	7	.0000
15	9	.0000	7	.0000	7	.0000

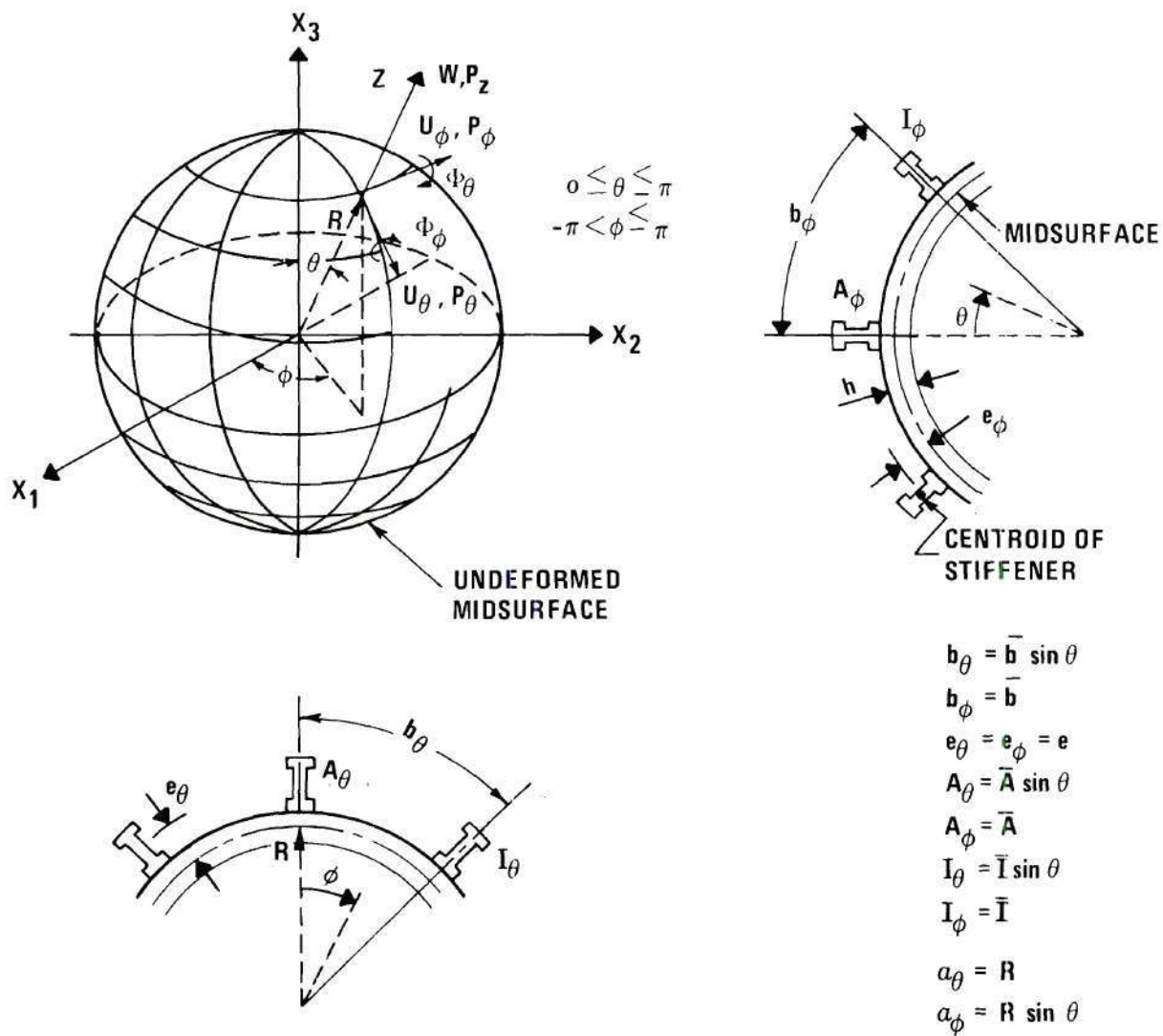


Figure 1. Geometry and Sign Convention.

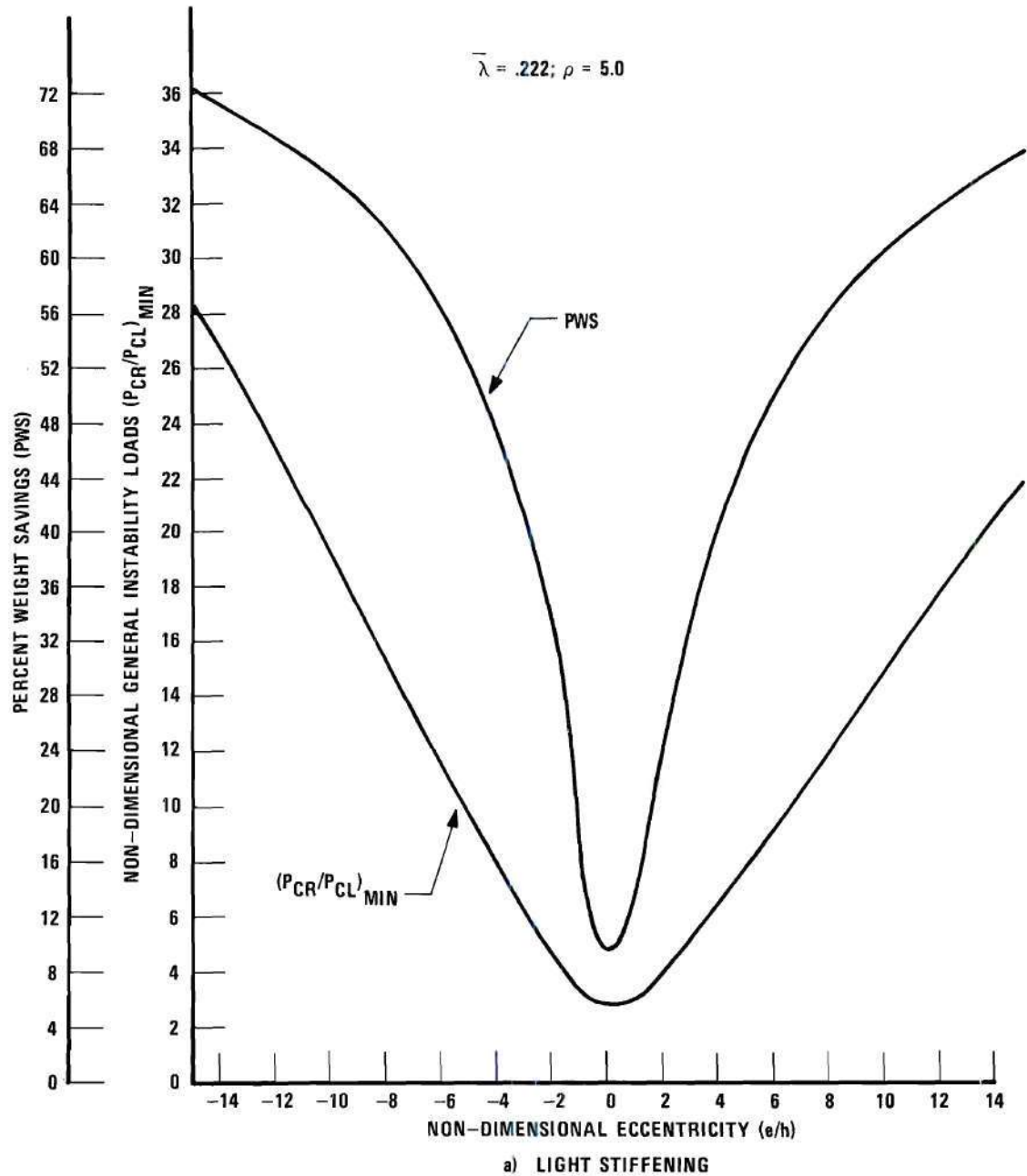


Figure 2. The Effect of Stiffner Eccentricity.

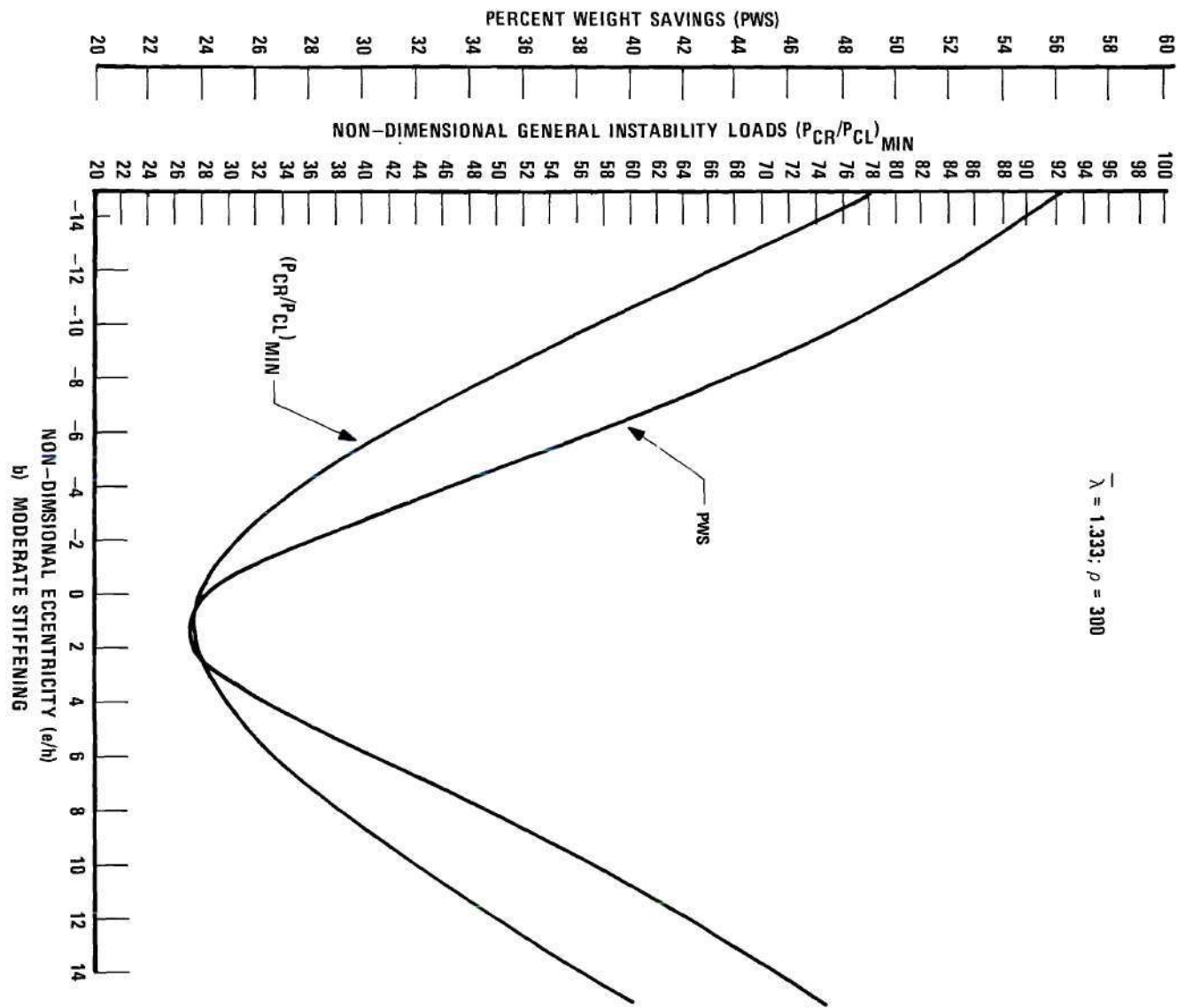


Figure 2. The Effect of Stiffener Eccentricity.

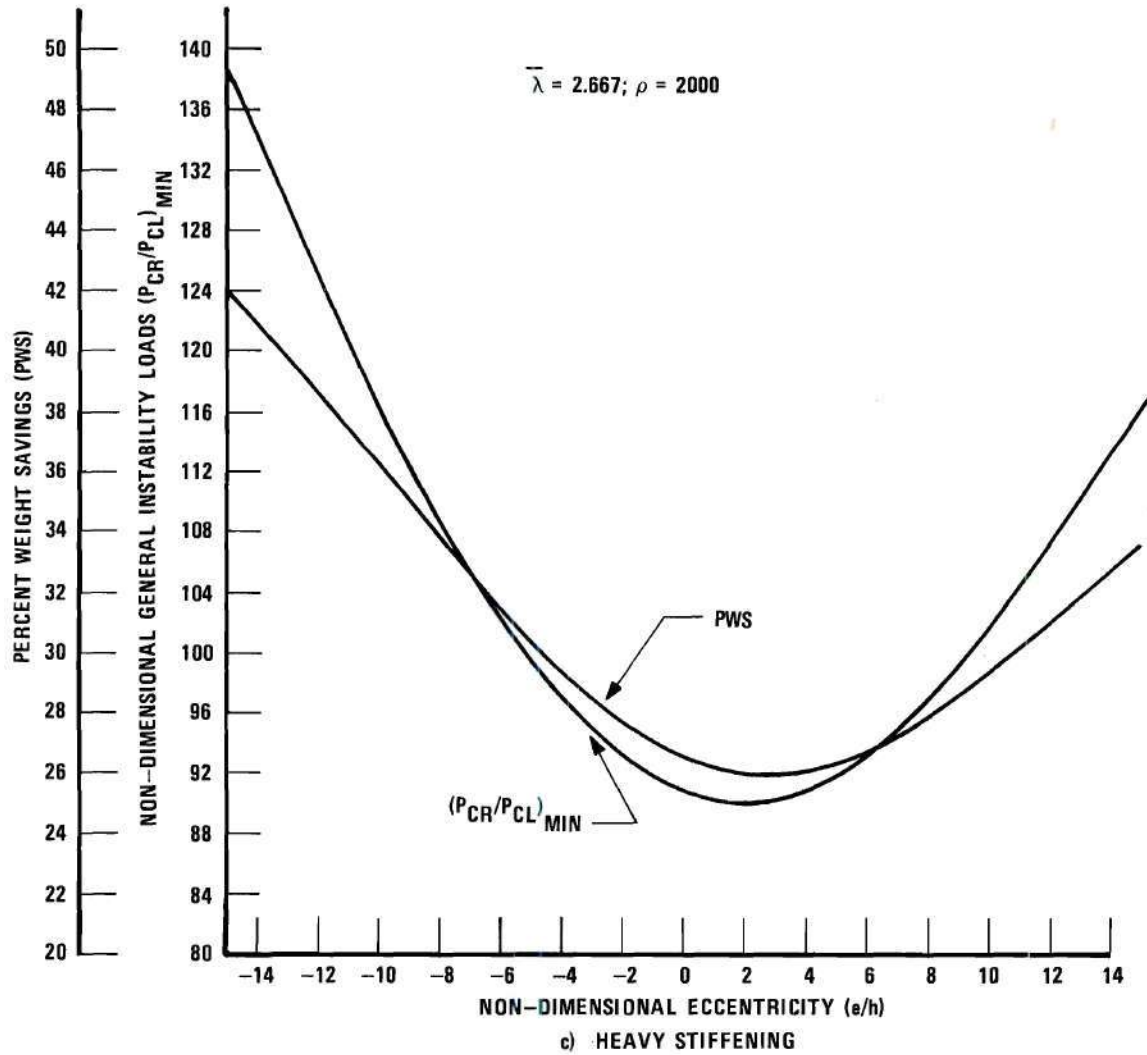


Figure 2. The Effect of Stiffener Eccentricity.

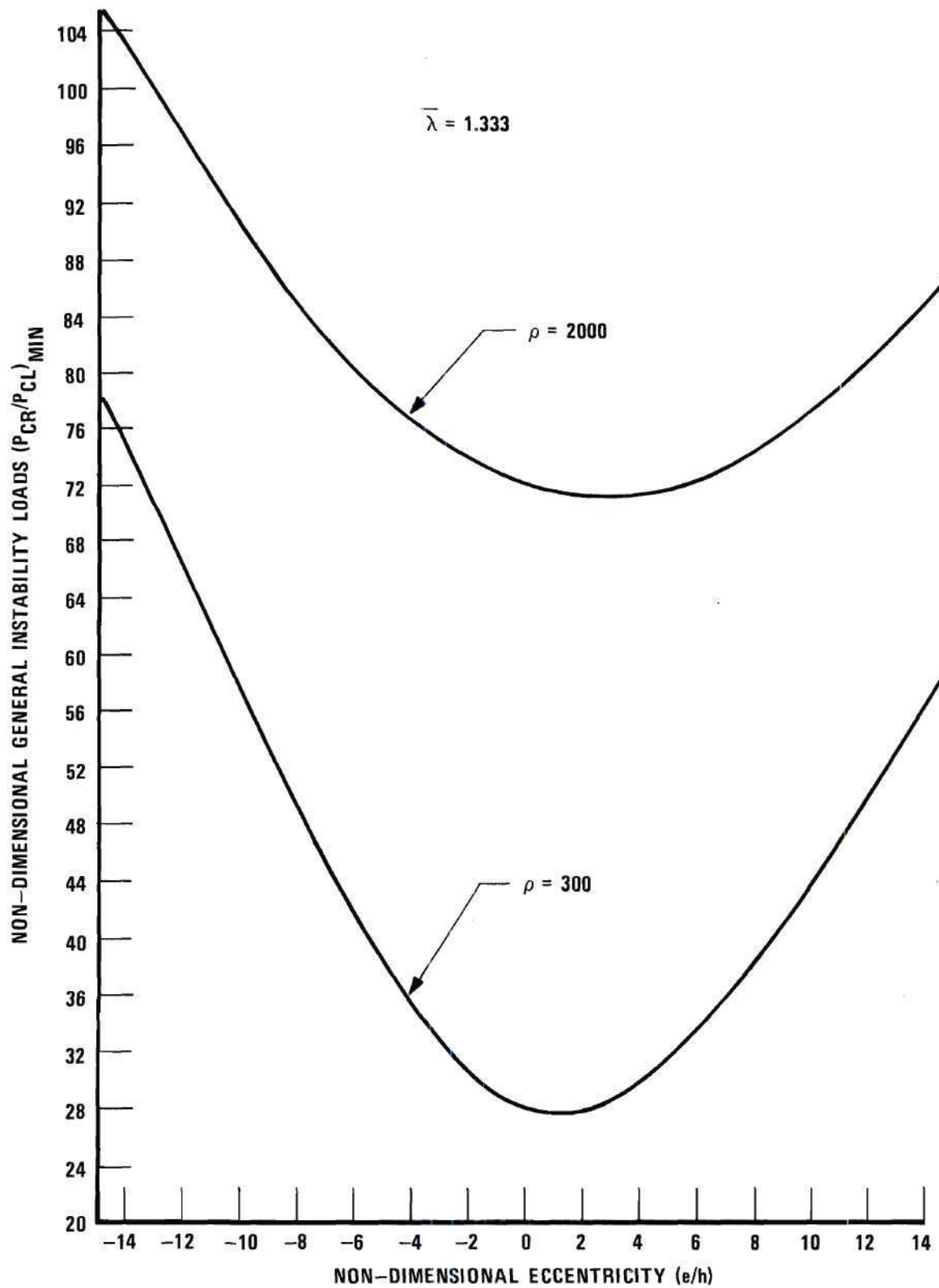


Figure 3. The Effect of ρ on the General Instability Loads.

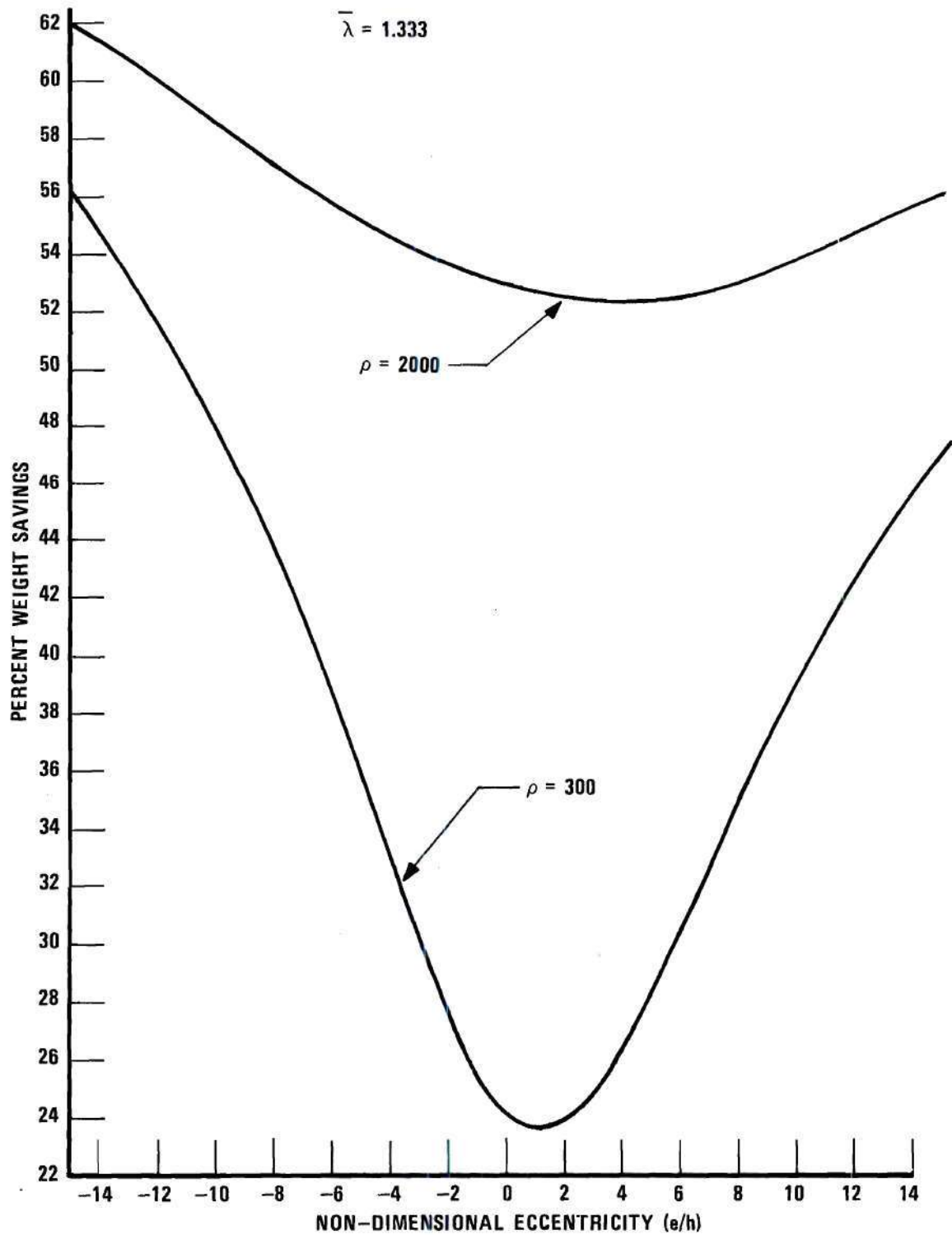


Figure 4. The Effect of ρ on the Percent Weight Savings.

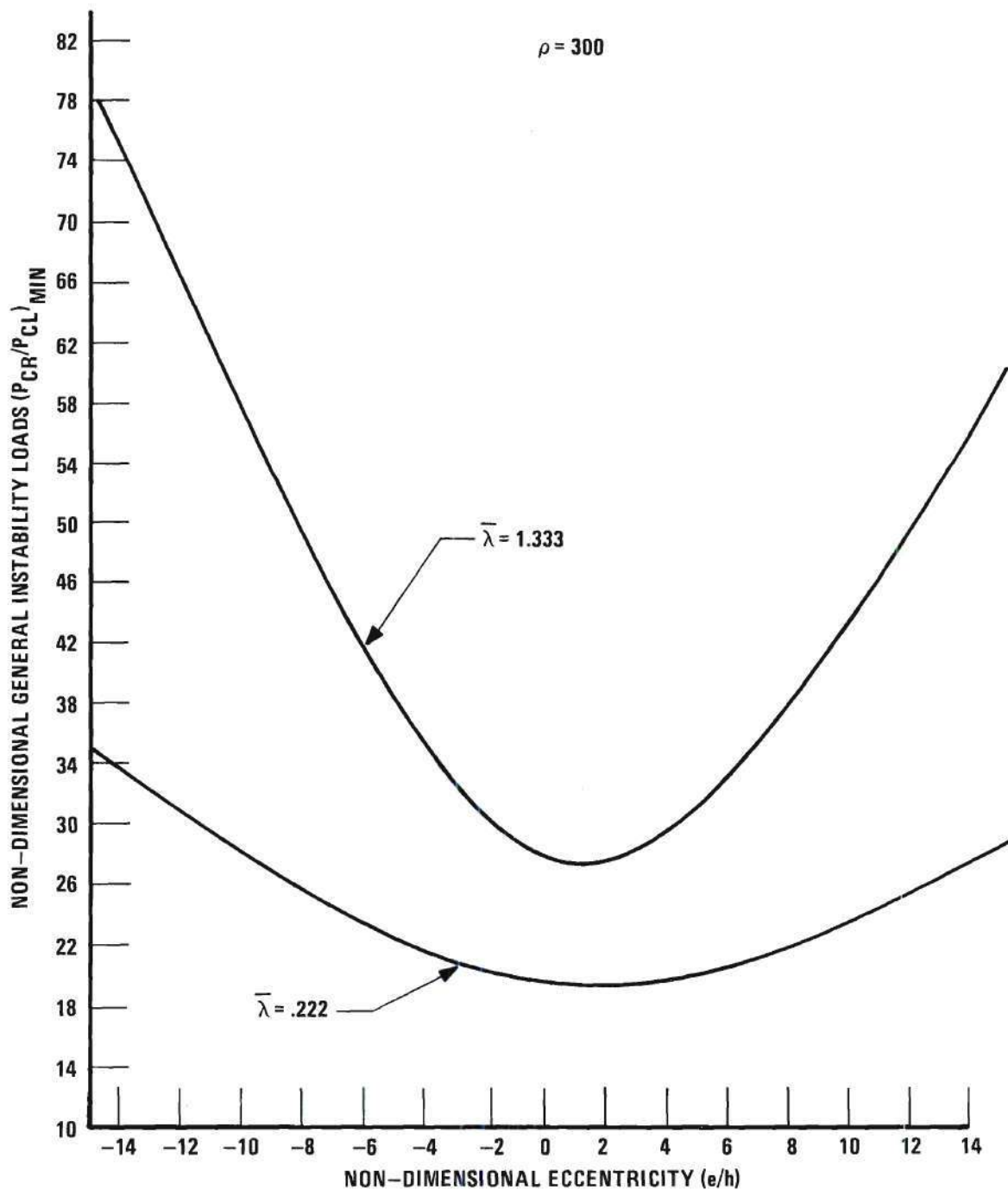


Figure 5. The Effect of $\bar{\lambda}$ on the General Instability Loads.

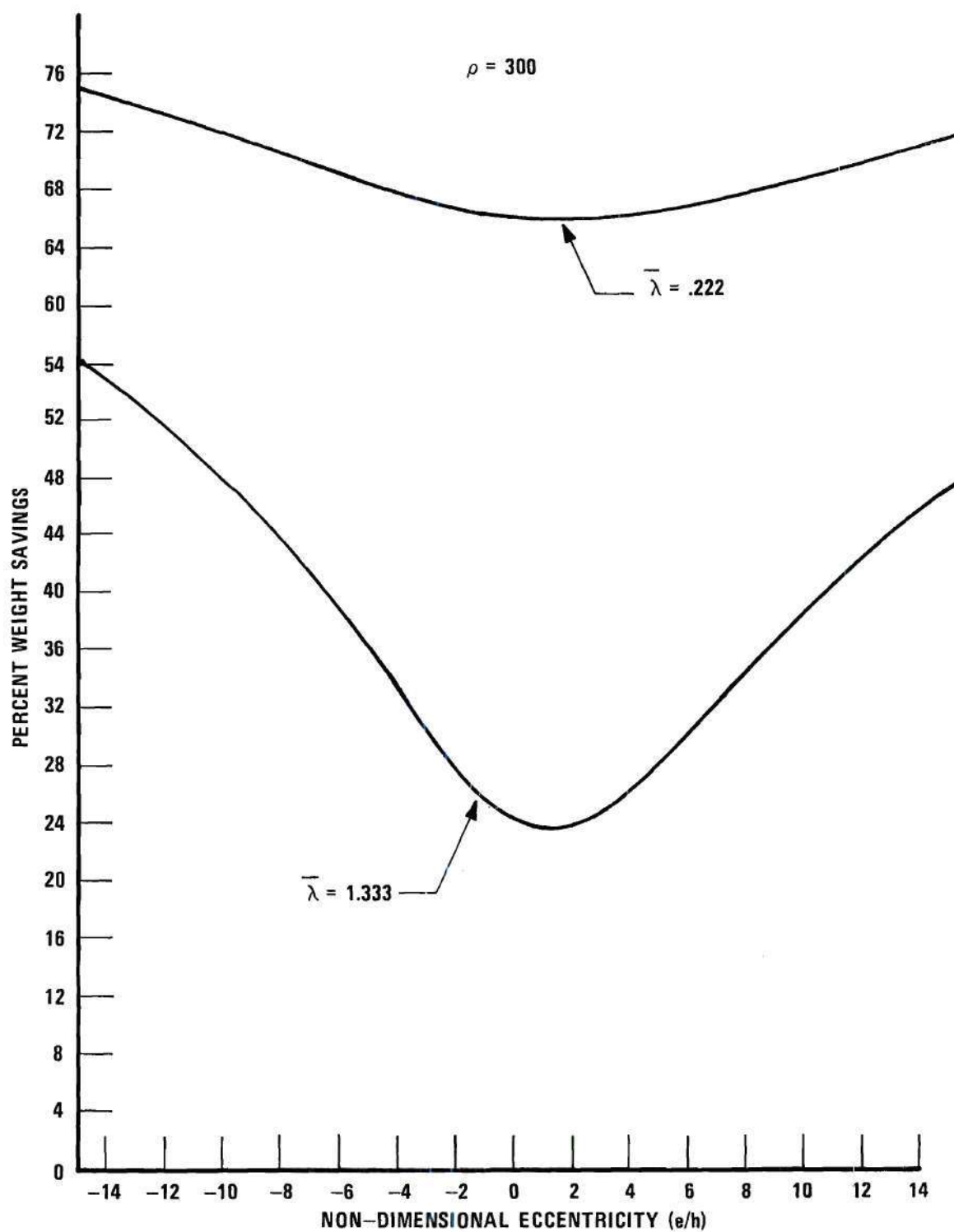


Figure 6. The Effect of $\bar{\lambda}$ on the Percent Weight Savings.

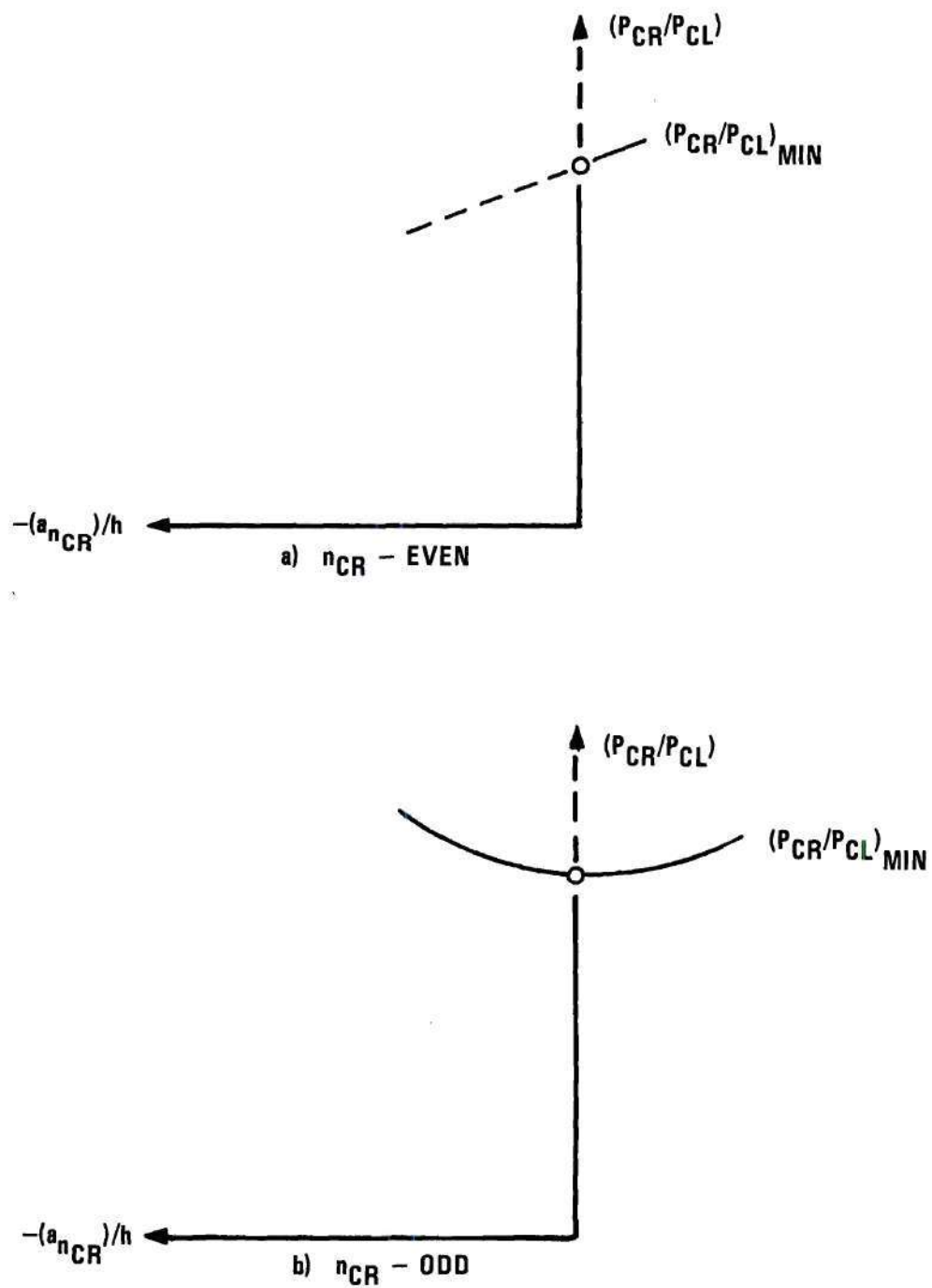


Figure 7. Initial Post-Buckling Behavior Suggested.

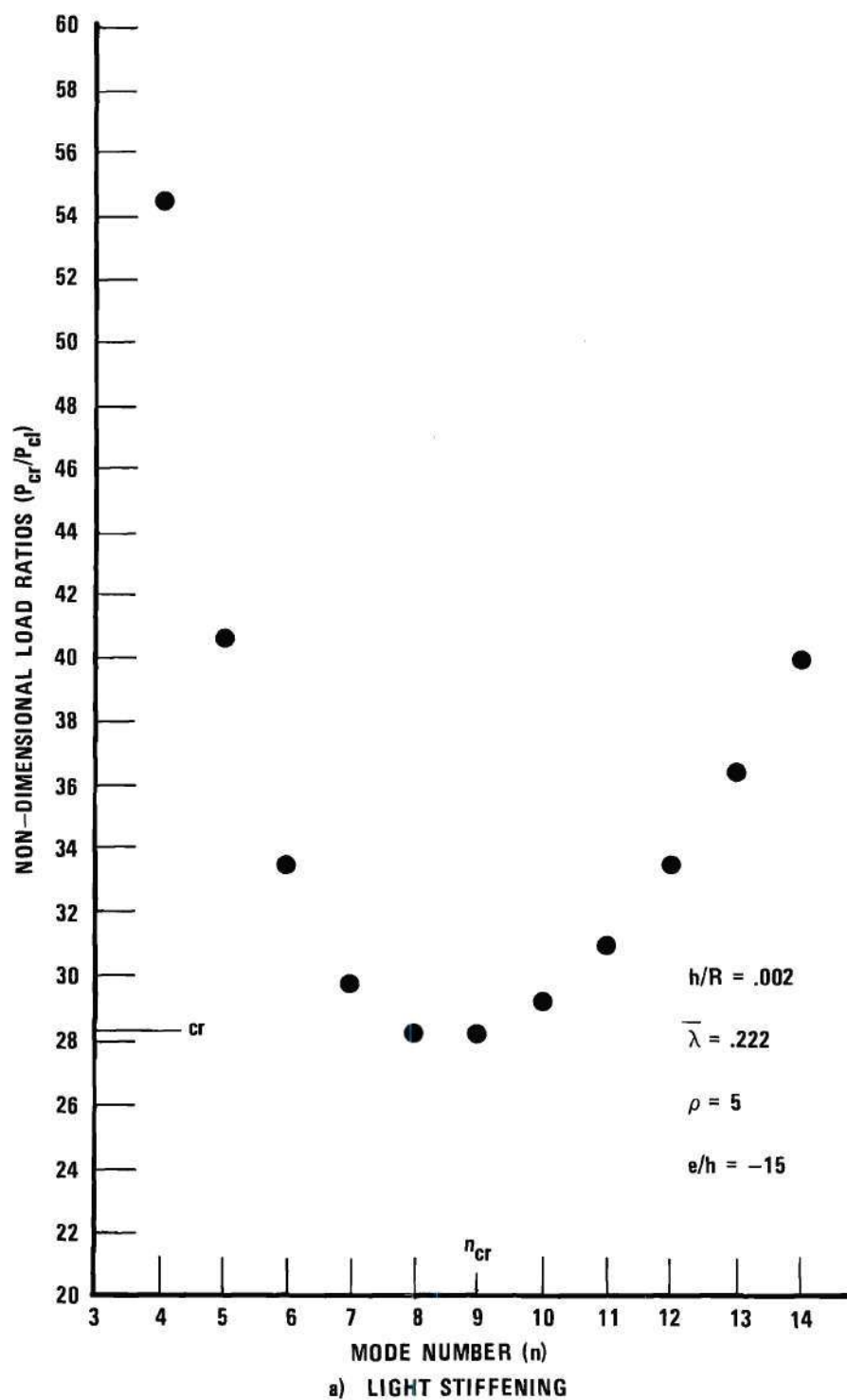


Figure 8. Spacing of the Bifurcation Points.

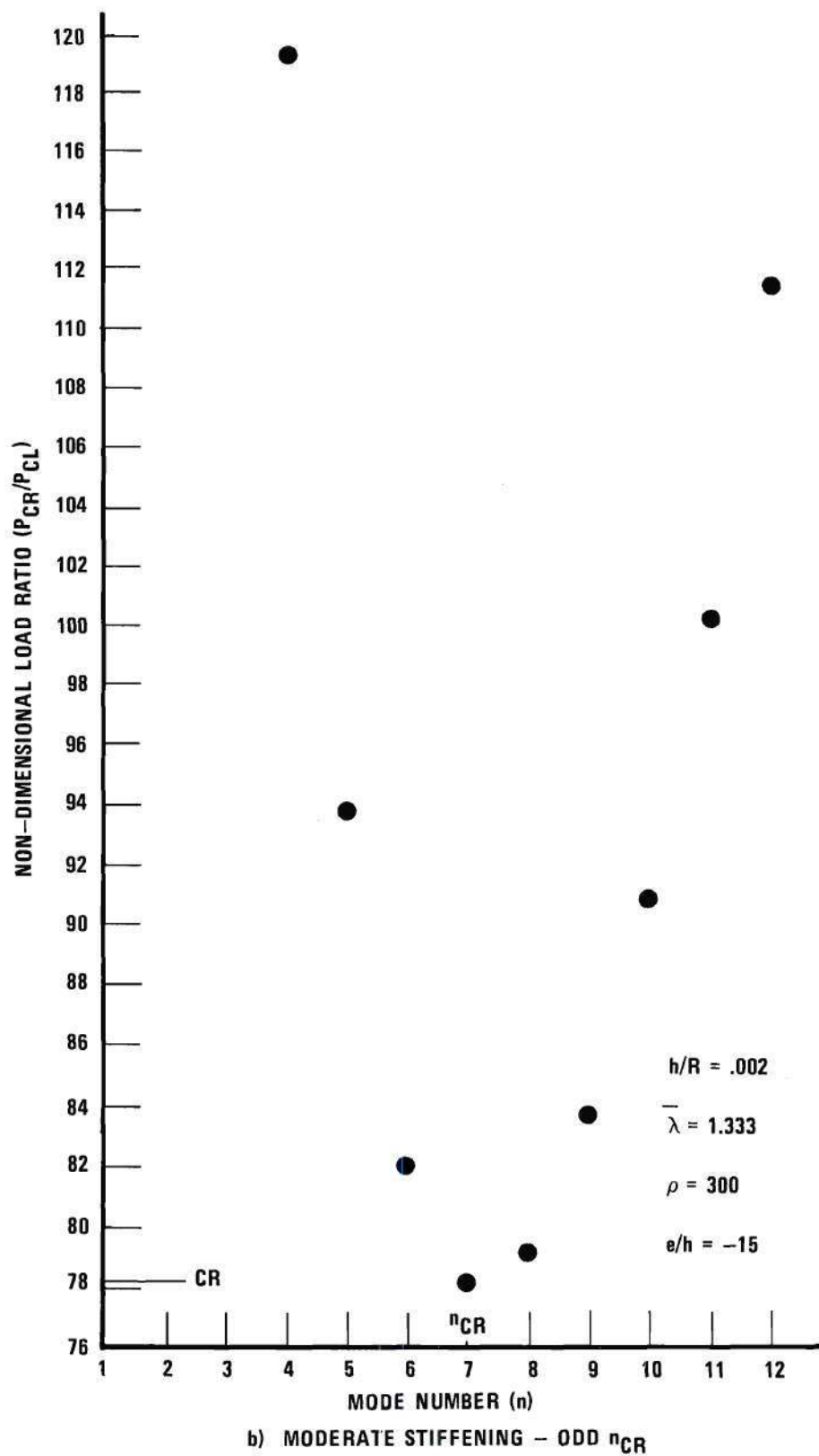


Figure 8. Spacing of the Bifurcation Points.

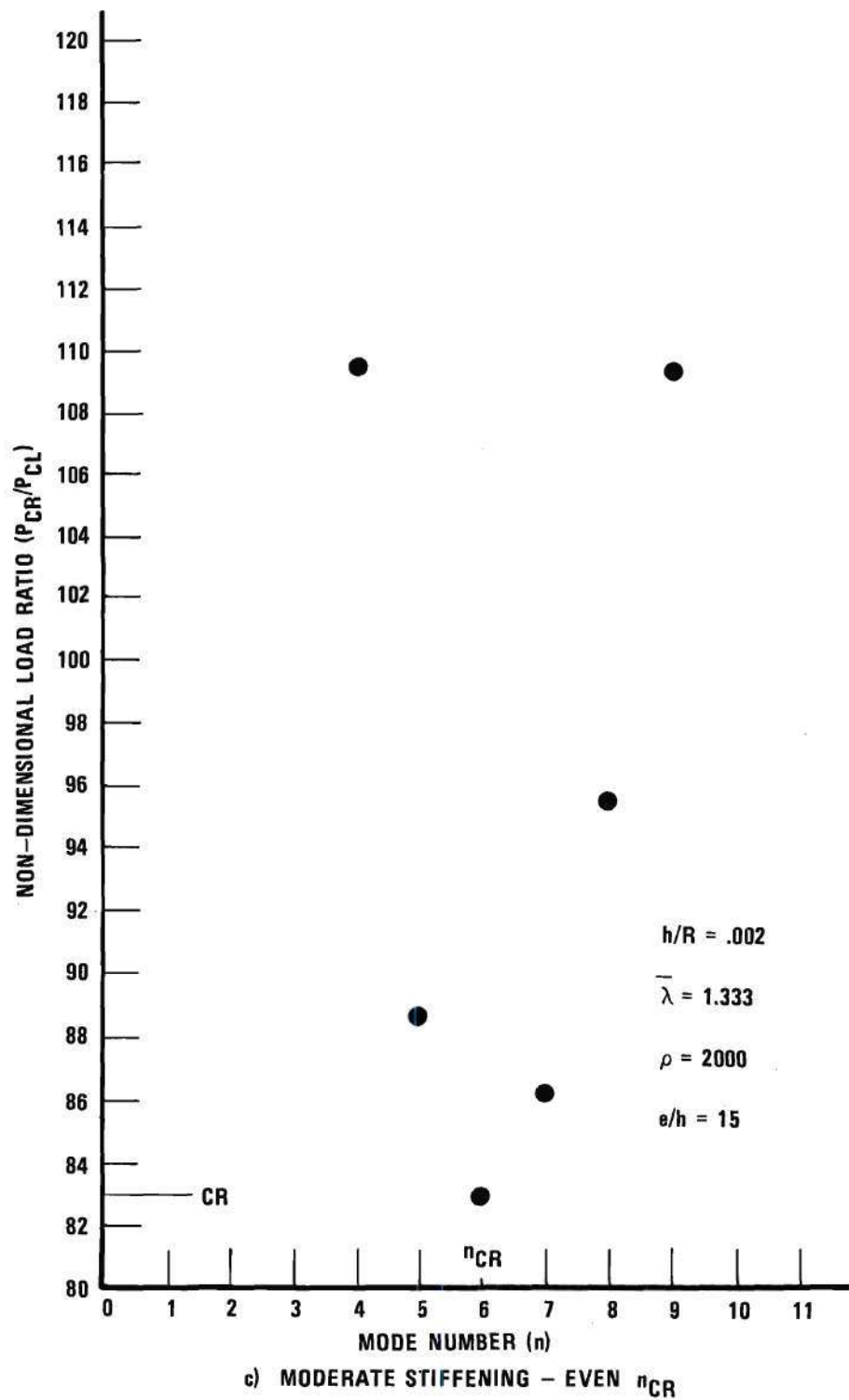


Figure 8. Spacing of the Bifurcation Points.

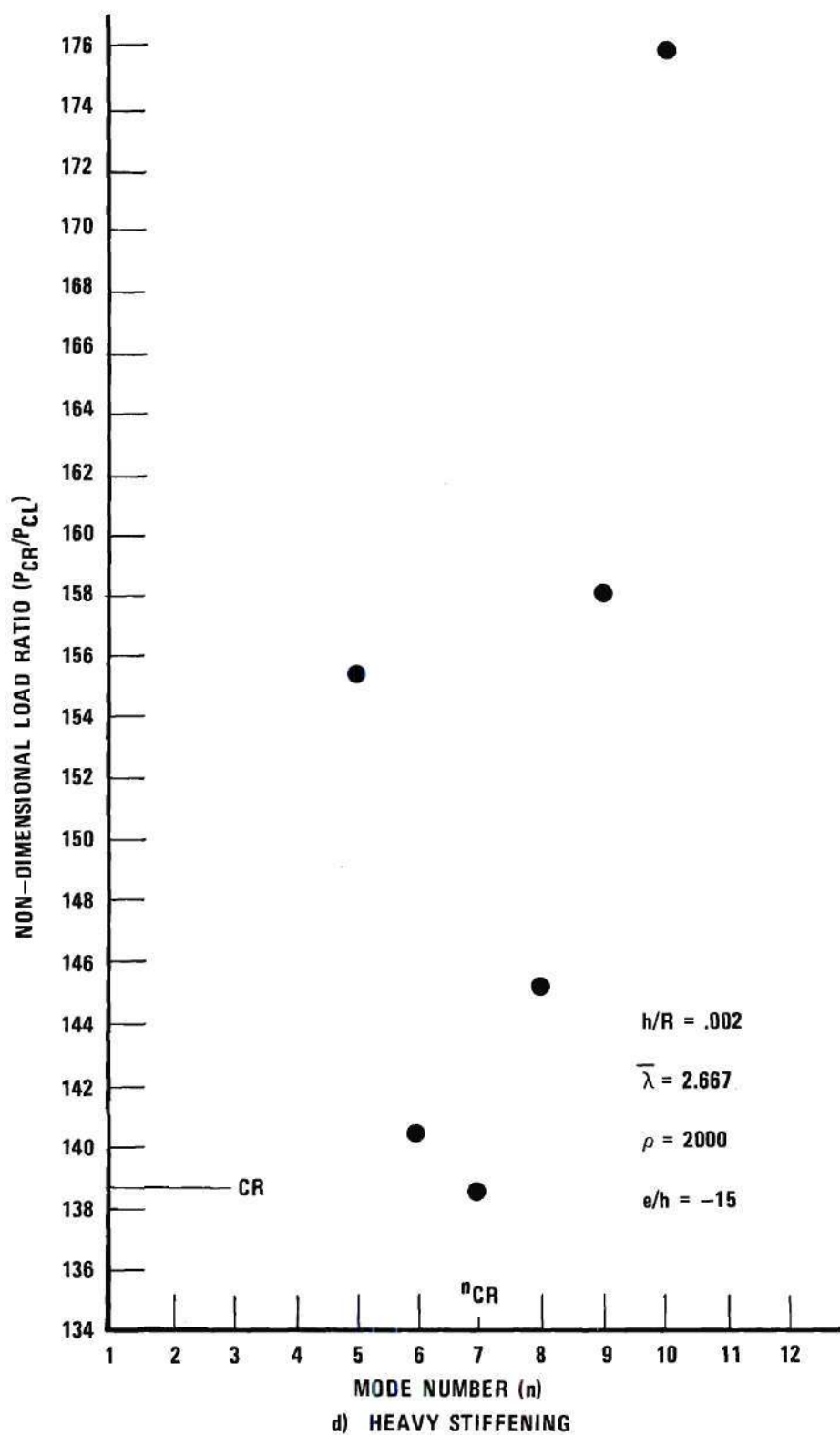


Figure 8. Spacing of the Bifurcation Points.

APPENDIX

APPENDIX A

DERIVATION OF THE CRITICAL CONDITION

Let the following constants be defined:

$$\xi_1 = \bar{\lambda} \frac{e}{R} + \alpha^* (1+\rho) + \bar{\lambda} \frac{e^{2*}}{R^2} \quad (A-1)$$

$$\xi_2 = 1 + v + \bar{\lambda} \left(1 - \frac{e}{R} + \frac{e^*}{R} \right) - \alpha^* (1+\rho-v) - \bar{\lambda} \frac{e^{2*}}{R^2} + \beta \begin{pmatrix} 1^* \\ 1^* - 2 \\ 1^* \end{pmatrix} \quad (A-2)$$

$$\xi_3 = 1 + \bar{\lambda} \left(1 + \frac{e}{R} + \frac{e^*}{R} \right) + \alpha^* (1+\rho) + \bar{\lambda} \frac{e^{2*}}{R^2} \quad (A-3)$$

$$\xi_4 = 1 - v + \bar{\lambda} \left(1 + \frac{e}{R} + \frac{e^*}{R} \right) + \alpha^* (1+\rho-v) + \bar{\lambda} \frac{e^{2*}}{R^2} - \beta \begin{pmatrix} 1^* \\ 1^* - 2 \\ 1^* - 2 \end{pmatrix} \quad (A-4)$$

$$\xi_5 = \alpha(1+\rho) + \bar{\lambda} \frac{e^2}{R^2} \quad (A-5)$$

$$\xi_6 = \alpha(1+\rho-v) - 2\bar{\lambda} \frac{e}{R} + \bar{\lambda} \frac{e^2}{R^2} - \beta \quad (A-6)$$

$$\xi_7 = 2(1+\bar{\lambda}+v) \quad (A-7)$$

$$\xi_8 = \bar{\lambda} \frac{e}{R} + \alpha^* (1+\rho) + \bar{\lambda} \frac{e^{2*}}{R^2} \quad (A-8)$$

$$\xi_9 = 1 + v + \bar{\lambda} \left(1 - \frac{e}{R} + \frac{e^*}{R} \right) - \alpha^* (1 + \rho - v) - \bar{\lambda} \frac{e^{2*}}{R^2} + \beta^*. \quad (A-9)$$

The buckling Equations, Equations (19), can then be written as

$$(-\xi_1 \nabla^2 + \xi_2) W' + (\xi_3 \nabla^2 + \xi_4) S' = 0 \quad (A-10)$$

$$(-\xi_5 \nabla^4 - \xi_6 \nabla^2 - \xi_7) W' + (\xi_8 \nabla^4 - \xi_9 \nabla^2) S' = 0. \quad (A-11)$$

The Legendre polynomials satisfy the differential equation

$$\left[\frac{\partial^2}{\partial \theta^2} + \cot \theta \frac{\partial}{\partial \theta} + i(i+1) \right] P_i(\cos \theta) = 0 \quad (A-12)$$

and the associated Legendre functions satisfy the differential equation

$$\left[\frac{\partial^2}{\partial \theta^2} + \cot \theta \frac{\partial}{\partial \theta} - j^2 \csc^2 \theta + i(i+1) \right] P_i^j(\cos \theta) = 0. \quad (A-13)$$

With W' and S' defined by (20) and with the aid of (A-12) and (A-13)

it can be seen that

$$\nabla^2 W' = -i(i+1) W' \quad (A-14)$$

$$\nabla^2 S' = -i(i+1) S'. \quad (A-15)$$

Substitution of Equations (20) into Equation (A-10) and Equation (A-11) leads to the following equations:

$$\sum_{i=0}^{\infty} \{[\xi_1 i(i+1) + \xi_2]A_{0i} + [-\xi_3 i(i+1) + \xi_4]C_{0i}\}P_i(\cos \theta) \quad (A-16)$$

$$+ \sum_{i=1}^{\infty} \sum_{j=1}^i \{[\xi_1 i(i+1) + \xi_2][A_{ji} \cos j\phi + B_{ji} \sin j\phi] \\ + [-\xi_3 i(i+1) + \xi_4][C_{ji} \cos j\phi + D_{ji} \sin j\phi]\}P_i^j(\cos \theta) = 0$$

$$\sum_{i=0}^{\infty} \{-\xi_5 i^2(i+1)^2 + \xi_6 i(i+1) - \xi_7\}A_{0i} + [\xi_8 i^2(i+1)^2 \quad (A-17)$$

$$+ \xi_9 i(i+1)]C_{0i}\}P_i(\cos \theta) + \sum_{i=1}^{\infty} \sum_{j=1}^i \{[-\xi_5 i^2(i+1)^2 \\ + \xi_6 i(i+1) - \xi_7][A_{ji} \cos j\phi + B_{ji} \sin j\phi] + [\xi_8 i^2(i+1)^2 \\ + \xi_9 i(i+1)][C_{ji} \cos j\phi + D_{ji} \sin j\phi]\}P_i^j(\cos \theta) = 0$$

In order to clear Equation (A-16) and Equation (A-17) of the summations the following orthogonality relations are used:

$$\int_{-\pi}^{\pi} \cos m\phi \cos j\phi d\phi = \pi \delta_{jm} \quad (A-18)$$

$$\int_{-\pi}^{\pi} \sin m\phi \sin j\phi d\phi = \pi \delta_{jm} \quad (A-19)$$

$$\int_{-\pi}^{\pi} \cos m\phi \cos j\phi d\phi = 0 \quad (A-20)$$

$$\int_0^{\pi} \sin \theta P_n^m(\cos \theta) P_i^m(\cos \theta) d\theta = \quad (A-21)$$

$$\frac{2}{2n+1} \frac{(n+m)!}{(n-m)!} \delta_{in} \quad (A-21)$$

where

$$\delta_{in} = \begin{cases} 0 & i \neq n \\ 1 & i = n \end{cases} \quad (A-22)$$

Multiplication of Equation (A-16) and Equation (A-17) by $\sin \theta P_n(\cos \theta)$ and integration over the surface results in the relations

$$\{[\xi_1 n(n+1) + \xi_2]A_{on} + [-\xi_3 n(n+1) + \xi_4]C_{on}\} \frac{4}{2n+1} = 0 \quad (A-23)$$

$$[-\xi_5 n^2(n+1)^2 + \xi_6 n(n+1) - \xi_7]A_{on} \quad (A-24)$$

$$+ [\xi_8 n^2(n+1)^2 + \xi_9 n(n+1)]C_{on}\} \frac{4\pi}{2n+1} = 0$$

Multiplication of Equation (A-16) and Equation (A-17) by $\sin \theta \cos m\phi P_n^m(\cos \theta)$ and integration over the surface results in the relations

$$\{[\xi_1 n(n+1) + \xi_2]A_{mn} + [-\xi_3 n(n+1) + \xi_4]C_{mn}\} \frac{2\pi}{2n+1} \frac{(n+m)!}{(n-m)!} = 0 \quad (A-25)$$

$$\{[-\xi_5 n^2(n+1)^2 + \xi_6 n(n+1) - \xi_7]A_{mn} + [\xi_8 n^2(n+1)^2 \quad (A-26)$$

$$+ \xi_9 n(n+1)]C_{mn}\} \frac{2\pi}{2n+1} \frac{(n+m)!}{(n-m)!} = 0.$$

Multiplication of Equation (A-16) and Equation (A-17) by $\sin \theta \sin m\phi P_n^m(\cos \theta)$ and integration over the surface results in the relations

$$\{[\xi_1 n(n+1) + \xi_2]B_{mn} + [-\xi_3 n(n+1) + \xi_4]D_{mn}\} \frac{2\pi}{2n+1} \frac{(n+m)!}{(n-m)!} = 0 \quad (A-27)$$

$$\{[-\xi_5 n^2(n+1)^2 + \xi_6 n(n+1) - \xi_7]B_{mn} + [\xi_8 n^2(n+1)^2 \quad (A-28)$$

$$+ \xi_9 n(n+1)]D_{mn}\} \frac{2\pi}{2n+1} \frac{(n+m)!}{(n-m)!} = 0.$$

It is now easily seen that the critical condition, Equation (21), is obtained by the simultaneous solution of the algebraic equations

$$\{[\xi_1 n(n+1) + \xi_2]A + [-\xi_3 n(n+1) + \xi_4]B = 0 \quad (A-29)$$

$$\{[-\xi_5 n^2(n+1)^2 + \xi_6 n(n+1) - \xi_7]A + [\xi_8 n^2(n+1)^2 + \xi_9 n(n+1)]B = 0 \quad (A-30)$$

where

$$A = A_{on}, \quad A_{mn}, \quad \text{or} \quad B_{mn} \quad (A-31)$$

$$B = C_{on}, \quad C_{mn}, \quad \text{or} \quad D_{mn} \quad (A-32)$$

and that the assumption of axisymmetric deflections $[W' = a_{on} P_n(\cos \theta); S' = C_{on} P_n(\cos \theta)]$ would have given the same eigenvalues.

APPENDIX B

THE TWO PROGRAMS FROM THE LINEAR ANALYSIS

Making the Mushtari-Vlasov-Donnell Approximation

```

      READ(5,1)I
1  FORMAT(I4)
      DO 11 J=1,I
      READ(5,2)HR,BL,RO
2  FORMAT(E7.3,F6.3,F8.3)
HR  IS THE SHELL THICKNESS OVER THE RADIUS
BL  IS LAMDA BAR
RO  IS RHO
      WRITE(6,3)HR,BL,RO
3  FORMAT(1H1,5X,5HHR = ,E7.3,5X,5HBL = ,F6.3,5X,5HRO = ,F8.3///
      13X,2HEH,8X,2HN1.5X,4HSPR1.9X,2HN2,5X,4HSPR2,9X,2HN3,5X,4HSPR3,
      29X,4HPWS1,9X,4HPWS2,9X,4HPWS3///)
EH  IS THE STIFFENER ECCENTRICITY OVER THE SHELL THICKNESS
N1,N2,N3 ARE THE CRITICAL MODE NUMBERS FOR LOAD CASES 1,2,AND3 RESPECTIVELY
PWS1,PWS2,PWS3 ARE THE PERCENT WEIGHT SAVINGS
      DO 11 K=0,30
      EH=-15+K
      RH=1./HR
      ER=EH*HR
      AL=(HR**2)/12.
AL  IS ALPHA
      E1=(3./4.)*(SQRT(3./2.))*RH
      E2=(27./16.)*(RH**2)
      E3=BL*(1.+ER)
      E4=BL*(1.+3.*ER-2.*(ER**2))
      E5=AL*(1.+RO)
      E6=BL*(1.-7.*ER+2.*(ER**2))
      E7=AL*((2./3.)+RO)
      E8=2.*((4./3.)+BL)
      E9=BL*(1.+ER-2.*(ER**2))
      E10=BL*(1.+5.*ER-2.*(ER**2))
      E11=BL*ER*(-2.+ER)
      E12=1.+E4-2.*E5
      E13=2.+E6+2.*E7
      E14=1.+E9-2.*E5
      E15=-(2./3.)-E10+2.*E7
      E19=1.+(9./4.)*E3
      A1=0.
      A2=1.
      A3=1.

```



```

SPR1=1000.
SPR2=1000.
SPR3=1000.
DO 12 N=2,100
D1=N*(N+1)
E16=-(E5+BL*(ER**2))*D1+E7+E11-(E8/D1)
E17=(1.+E3)*D1-(2./3.)*E3
E18=BL*ER*D1+(4./3.)*BL*(1.-ER)
B1=E1*E17
B2=E1*(E12*D1+E13+2.*(E8/D1))
B3=E1*(E14*D1+E15+2.*(E8/D1))
C=E2*(E16*E17+(E18**2))
PR1=-C/B1
PR2=(-B2+SQRT((B2**2)-4.*A2*C))/(2.*A2)
PR3=(-B3+SQRT((B3**2)-4.*A3*C))/(2.*A3)
IF(PR1-SPR1)4,5,5
4 SPR1=PR1
N1=N
5 CONTINUE
IF(PR2-SPR2)6,7,7
6 SPR2=PR2
N2=N
7 CONTINUE
IF(PR3-SPR3)8,9,9
8 SPR3=PR3
N3=N
9 CONTINUE
12 CONTINUE
PWS1=(1.-(E19/SQRT(SPR1)))*100.
PWS2=(1.-(E19/SQRT(SPR2)))*100.
PWS3=(1.-(E19/SQRT(SPR3)))*100.
WRITE(6,10)EH,N1,SPR1,N2,SPR2,N3,SPR3,PWS1,PWS2,PWS3
10 FORMAT(3X,F7.3,3X,3(I4,3X,E9.3,3X),3(E9.3,3X))
11 CONTINUE
END

```

Not Making the Mushtari-Vlasov-Donnell Approximation

```

      READ(5,1)I
1  FORMAT(I4)
      DO 11 J=1,I
        READ(5,2)HR,BL,RO
2  FORMAT(E7.3,F6.3,F8.3)
HR IS THE THICKNESS OVER THE RADIUS
BL IS LAMDA BAR
RO IS RHO
      WRITE(6,3)HR,BL,RO
3  FORMAT(1H1,5X,5HHR = ,E7.3,5X,5HBL = ,F6.3,5X,5HRO = ,F8.3///
13X,2HEH,8X,2HN1,5X,4HSPR1,9X,2HN2,5X,4HSPR2,9X,2HN3,5X,4HSPR3,
29X,4HPWS1,9X,4HPWS2,9X,4HPWS3///)
EH IS THE STIFFENER ECCENTRICITY OVER THE SHELL THICKNESS
N1,N2,N3 ARE THE CRITICAL MODE NUMBERS FOR LOAD CASES 1,2,3 RESPECTIVELY
SPR1,SPR2,SPR3 ARE THE NON-DIMENSIONAL GENERAL INSTABILITY LOADS
PWS1,PWS2,PWS3 ARE THE PERCENT WEIGHT SAVINGS
      DO 11 K=0,30
        EH=-15+K
        RH=1./HR
        ER=EH*HR
        AL=(HR**2)/12.
AL IS ALPHA
        E1=(3./4.)*(SQRT(3./2.))*RH
        E2=(27./16.)*(RH**2)
        E3=-(10./3.)-3.*BL
        E4=2.*((4./3.)+BL)
        E5=-(2./3.)-BL*(1.+4.*ER)
        E6=AL*(1.+RO)
        E7=AL*((2./3.)+RO)
        E8=BL*ER*(-2.+ER)
        E9=BL*((1.+ER)**2)
        E10=BL*ER*(1.+ER)
        E11=(4./3.)+BL*(1.-(ER**2))
        E12=1.+BL*(1.+2.*ER)
        E13=1.+BL*(1.-2.*(ER**2))-2.*E6
        E14=E3+2.*(E7+E8)
        E15=-(2./3.)-E9-E7
        E19=1.+(9./4.)*BL*(1.+ER)
        A1=0.
        A2=0.
        A3=1.
        SPR1=1000.
        SPR2=1000.
        SPR3=1000.
      DO 12 N=2,100
        D1=N*(N+1)
        E16=-(E6+BL*(ER**2))*D1+E7+E8-(E4/D1)
        E17=(1.+E9+E6)*D1+E15
        E18=(E10+E6)*D1+E11-E7

```

```

B=B1/B2
D3=N1
E8=2./(2.*D3+1.)
E9=(-2.*(B**2)+4.*B+1.)*D2
E10=-(8.*(SQRT(2.))*HR*SPR)/9.
E11=(B**2)*(B-(3./2.))*D2+B*(-B+2)-(4./(3.*D2))
E12=(SQRT(3.)/3.)*BL*(B-ER)*D2
CN1=E8*(E9-4.)
IF((INT(N1/2))*2-N1)6,7,7
6 DN1=0.
GO TO 9
7 DN1=E10*E11+E12+E13
9 E7=9.*(SQRT(3.))/(4.*(SQRT(2.))*3.1415927*SPR)
SL=E7*(DN1/CN1)
SL IS THE INITIAL POST-BUCKLING SLOPE
WRITE(6,10)EH,N1,SPR,PWS,SL
10 FORMAT(3X,F7.3,3X,I4,3X,E10.5,3X,E10.5,3X,E9.3)
11 CONTINUE
END

```

APPENDIX C

REDUCTION OF THE ENERGY FUNCTIONALS

The evaluation of $P_3^0 \left[\frac{u_{CR}}{a_{n_{CR}}}, \frac{W_{1_{CR}}}{a_{n_{CR}}} \right]$ is presented as typical starting with Equation (51b). Substitution of the buckling modes gives

$$P_3^0 \left[\frac{u_{CR}}{a_{n_{CR}}}, \frac{W_{1_{CR}}}{a_{n_{CR}}} \right] = \frac{\pi E h}{R(1-\nu^2)} (B^3 \int_0^\pi \{-2\beta_{CR} \cos^3 \theta \left[\frac{\partial}{\partial \theta} P_{n_{CR}}(\cos \theta) \right]^3 \quad (C-1)$$

$$- 2\beta_{CR} \sin \theta \cos^2 \theta \left[\frac{\partial}{\partial \theta} P_{n_{CR}}(\cos \theta) \right]^2 \left[\frac{\partial^2}{\partial \theta^2} P_{n_{CR}}(\cos \theta) \right] \} d\theta$$

$$+ B^2 \int_0^\pi \{-6\beta_{CR} \sin \theta \cos^2 \theta P_{n_{CR}}(\cos \theta) \left[\frac{\partial}{\partial \theta} P_{n_{CR}}(\cos \theta) \right]^2$$

$$- 4\beta_{CR} \sin^2 \theta \cos \theta P_{n_{CR}}(\cos \theta) \left[\frac{\partial}{\partial \theta} P_{n_{CR}}(\cos \theta) \right] \left[\frac{\partial^2}{\partial \theta^2} P_{n_{CR}}(\cos \theta) \right]$$

$$+ 2\beta_{CR} \cos^3 \theta \left[\frac{\partial}{\partial \theta} P_{n_{CR}}(\cos \theta) \right]^3 \} d\theta + B \int_0^\pi \{-6\beta_{CR} \sin^2 \theta \cdot$$

$$\cos \theta [P_{n_{CR}}(\cos \theta)]^2 \left[\frac{\partial}{\partial \theta} P_{n_{CR}}(\cos \theta) \right] - 2\beta_{CR} \sin^3 \theta [P_{n_{CR}}(\cos \theta)]^2 \cdot$$

$$\left[\frac{\partial^2}{\partial \theta^2} P_{n_{CR}}(\cos \theta) \right] + 4\beta_{CR} \sin \theta \cos^2 \theta P_{n_{CR}}(\cos \theta) \cdot$$

$$\left[\frac{\partial}{\partial \theta} P_{n_{CR}}(\cos \theta) \right]^2 + (1+\bar{\lambda}) \sin \theta \left[\frac{\partial}{\partial \theta} P_{n_{CR}}(\cos \theta) \right]^2 \cdot$$

$$\begin{aligned}
& \left[\frac{\partial^2}{\partial \theta^2} P_{n_{CR}}(\cos \theta) \right] + v \cos \theta \left[\frac{\partial}{\partial \theta} P_{n_{CR}}(\cos \theta) \right]^3 \} d\theta + \int_0^\pi \{ -2\beta_{CR} \sin^3 \theta \cdot \\
& [P_{n_{CR}}(\cos \theta)]^3 + 2\beta_{CR} \sin^2 \theta \cos \theta [P_{n_{CR}}(\cos \theta)]^2 \left[\frac{\partial}{\partial \theta} P_{n_{CR}}(\cos \theta) \right] \\
& + (1+\bar{\lambda}+v) \sin \theta P_{n_{CR}}(\cos \theta) \left[\frac{\partial}{\partial \theta} P_{n_{CR}}(\cos \theta) \right]^2 \\
& - \bar{\lambda} \frac{e}{R} \sin \theta \left[\frac{\partial}{\partial \theta} P_{n_{CR}}(\cos \theta) \right]^2 \left[\frac{\partial^2}{\partial \theta^2} P_{n_{CR}}(\cos \theta) \right] \} d\theta \} .
\end{aligned}$$

Using integration by parts as indicated below gives

$$\begin{aligned}
& \int_0^\pi \cos^2 \theta \sin \theta \left[\frac{\partial}{\partial \theta} P_{n_{CR}}(\cos \theta) \right]^2 \left[\frac{\partial^2}{\partial \theta^2} P_{n_{CR}}(\cos \theta) \right] d\theta \quad (C-2) \\
& = \frac{1}{3} \int_0^\pi \frac{u}{\cos^2 \theta \sin \theta} \frac{dv}{\frac{\partial}{\partial \theta} \left[\frac{\partial}{\partial \theta} P_{n_{CR}}(\cos \theta) \right]^3} d\theta = - \int_0^\pi \cos^3 \theta \cdot \\
& \left[\frac{\partial}{\partial \theta} P_{n_{CR}}(\cos \theta) \right]^3 d\theta + \frac{2}{3} \int_0^\pi \cos \theta \left[\frac{\partial}{\partial \theta} P_{n_{CR}}(\cos \theta) \right]^3 d\theta
\end{aligned}$$

$$\begin{aligned}
& \int_0^\pi \sin^2 \theta \cos \theta P_{n_{CR}}(\cos \theta) \left[\frac{\partial}{\partial \theta} P_{n_{CR}}(\cos \theta) \right] \left[\frac{\partial^2}{\partial \theta^2} P_{n_{CR}}(\cos \theta) \right] d\theta \quad (C-3) \\
& = \frac{1}{2} \int_0^\pi \frac{u}{\sin^2 \theta \cos \theta P_{n_{CR}}(\cos \theta)} \frac{\partial}{\partial \theta} \left[\frac{\partial}{\partial \theta} P_{n_{CR}}(\cos \theta) \right]^2 d\theta \\
& = \frac{1}{2} \int_0^\pi \cos^3 \theta \left[\frac{\partial}{\partial \theta} P_{n_{CR}}(\cos \theta) \right]^3 d\theta - \frac{3}{2} \int_0^\pi \cos^2 \theta \sin \theta \cdot \\
& P_{n_{CR}}(\cos \theta) \left[\frac{\partial}{\partial \theta} P_{n_{CR}}(\cos \theta) \right]^2 d\theta - \frac{1}{2} \int_0^\pi \cos \theta \left[\frac{\partial}{\partial \theta} P_{n_{CR}}(\cos \theta) \right]^3 d\theta \\
& + \frac{1}{2} \int_0^\pi \sin \theta P_{n_{CR}}(\cos \theta) \left[\frac{\partial}{\partial \theta} P_{n_{CR}}(\cos \theta) \right]^2 d\theta
\end{aligned}$$

$$\int_0^{\pi} \sin \theta \cos^2 \theta P_{n_{CR}}(\cos \theta) \left[\frac{\partial}{\partial \theta} P_{n_{CR}}(\cos \theta) \right]^2 d\theta \quad (C-4)$$

$$= \frac{1}{2} \int_0^{\pi} \frac{u}{\sin \theta \cos^2 \theta \left[\frac{\partial}{\partial \theta} P_{n_{CR}}(\cos \theta) \right]} \frac{dv}{\frac{\partial}{\partial \theta} [P_{n_{CR}}(\cos \theta)]^2} d\theta$$

$$= \frac{1}{2} \int_0^{\pi} \sin^3 \theta [P_{n_{CR}}(\cos \theta)]^2 \left[\frac{\partial^2}{\partial \theta^2} P_{n_{CR}}(\cos \theta) \right] d\theta$$

$$+ \frac{3}{2} \int_0^{\pi} \cos \theta \sin^2 \theta [P_{n_{CR}}(\cos \theta)]^2 \left[\frac{\partial}{\partial \theta} P_{n_{CR}}(\cos \theta) \right] d\theta$$

$$+ \frac{1}{2} n_{CR}(n_{CR}+1) \int_0^{\pi} \sin \theta [P_{n_{CR}}(\cos \theta)]^3 d\theta$$

$$\int_0^{\pi} \sin^2 \theta \cos \theta [P_{n_{CR}}(\cos \theta)]^2 \left[\frac{\partial}{\partial \theta} P_{n_{CR}}(\cos \theta) \right] d\theta \quad (C-5)$$

$$= \frac{1}{3} \int_0^{\pi} \frac{u}{\sin^2 \theta \cos \theta} \frac{dv}{\frac{\partial}{\partial \theta} [P_{n_{CR}}(\cos \theta)]^3} d\theta$$

$$= \frac{2}{3} \int_0^{\pi} \sin \theta [P_{n_{CR}}(\cos \theta)]^3 d\theta + \int_0^{\pi} \sin^3 \theta [P_{n_{CR}}(\cos \theta)]^3 d\theta$$

Substitution of (C-2) through (C-5) into (C-1) gives

$$P_3^0 \left[\frac{u_{CR}}{a_{n_{CR}}}, \frac{w_{1CR}}{a_{n_{CR}}} \right] = \frac{\pi E h}{R(1-\nu^2)} \{ B^3 \int_0^{\pi} \left\{ -\frac{4}{3} \beta_{CR} \cos \theta \left[\frac{\partial}{\partial \theta} P_{n_{CR}}(\cos \theta) \right]^3 \right\} d\theta \quad (C-6)$$

$$+ B^2 \int_0^{\pi} \{ 2\beta_{CR} \cos \theta \left[\frac{\partial}{\partial \theta} P_{n_{CR}}(\cos \theta) \right]^3 - 2\beta_{CR} \sin \theta P_{n_{CR}}(\cos \theta) \cdot$$

$$\left[\frac{\partial}{\partial \theta} P_{n_{CR}}(\cos \theta) \right]^2 \} d\theta + B \int_0^{\pi} \{ 2\beta_{CR} n_{CR}(n_{CR}+1) \sin \theta [P_{n_{CR}}(\cos \theta)]^3$$

$$\begin{aligned}
& + (1+\bar{\lambda})\sin \theta \left[\frac{\partial}{\partial \theta} P_{n_{CR}}(\cos \theta) \right]^2 \left[\frac{\partial^2}{\partial \theta^2} P_{n_{CR}}(\cos \theta) \right] \\
& + v \cos \theta \left[\frac{\partial}{\partial \theta} P_{n_{CR}}(\cos \theta) \right]^3 d\theta \\
& + \int_0^\pi \left\{ -\frac{4}{3} \beta_{CR} \sin \theta \left[P_{n_{CR}}(\cos \theta) \right]^3 + (1+\bar{\lambda}+v)\sin \theta P_{n_{CR}}(\cos \theta) \cdot \right. \\
& \quad \left. \left[\frac{\partial}{\partial \theta} P_{n_{CR}}(\cos \theta) \right]^2 - \bar{\lambda} \frac{e}{R} \sin \theta \cdot \right. \\
& \quad \left. \left[\frac{\partial}{\partial \theta} P_{n_{CR}}(\cos \theta) \right]^2 \left[\frac{\partial^2}{\partial \theta^2} P_{n_{CR}}(\cos \theta) \right] \right\} d\theta
\end{aligned}$$

Again using integration by parts as indicated gives

$$\int_0^\pi \sin \theta P_{n_{CR}}(\cos \theta) \left[\frac{\partial}{\partial \theta} P_{n_{CR}}(\cos \theta) \right]^2 d\theta = \frac{1}{2} \int_0^\pi \frac{u}{\sin \theta \left[\frac{\partial}{\partial \theta} P_{n_{CR}}(\cos \theta) \right]} d\theta \quad (C-7)$$

$$\frac{dv}{\frac{\partial}{\partial \theta} \left[P_{n_{CR}}(\cos \theta) \right]^2 d\theta} = \frac{1}{2} n_{CR}(n_{CR}+1) \int_0^\pi \sin \theta \left[P_{n_{CR}}(\cos \theta) \right]^3 d\theta$$

$$\int_0^\pi \sin \theta \left[\frac{\partial}{\partial \theta} P_{n_{CR}}(\cos \theta) \right]^2 \left[\frac{\partial^2}{\partial \theta^2} P_{n_{CR}}(\cos \theta) \right] d\theta = \frac{1}{3} \int_0^\pi \frac{u}{\sin \theta} d\theta \quad (C-8)$$

$$\frac{dv}{\frac{\partial}{\partial \theta} \left[\frac{\partial}{\partial \theta} P_{n_{CR}}(\cos \theta) \right]^3 d\theta} = -\frac{1}{3} \int_0^\pi \cos \theta \left[\frac{\partial}{\partial \theta} P_{n_{CR}}(\cos \theta) \right]^3 d\theta$$

$$\int_0^\pi \frac{u}{\left[\frac{\partial}{\partial \theta} P_{n_{CR}}(\cos \theta) \right]^3} \frac{dv}{\cos \theta d\theta} = -\frac{3}{4} n_{CR}^2 (n_{CR}+1)^2 \int_0^\pi \sin \theta \left[P_{n_{CR}}(\cos \theta) \right]^3 d\theta \quad (C-9)$$

Substitution of (C-7) through (C-9) into (C-6) gives Equation (72).

APPENDIX D

THE PROGRAM FOR THE IMPERFECTION-SENSITIVITY STUDY

```

      READ(5,1)I
1  FORMAT(I4)
      DO 11 J=1,I
      READ(5,2)HR,BL,RO
2  FORMAT(E7.3,F6.3,F8.3)
HR IS THE SHELL THICKNESS OVER THE RADIUS
BL IS LAMDA BAR
RO IS RHO
      WRITE(6,3)HR,BL,RO
3  FORMAT(1H1,5X,5HHR = ,E7.3,5X,5HBL = ,F6.3,5X,5HRO = ,F8.3///
15X,2HEH,8X,2HN1,9X,3HSPR,9X,3HPWS,9X,2HSL///)
EH IS THE STIFFENER ECCENTRICITY OVER THE SHELL THICKNESS
N1 IS THE CRITICAL MODE NUMBER
SPR IS THE NON-DIMENSIONAL GENERAL INSTABILITY LOAD
PWS IS THE PERCENT WEIGHT SAVINGS
      DO 11 K=0,30
      EH=-15+K
      RH=1./HR
      ER=EH*HR
      AL=(HR**2)/12.
AL IS ALPHA
      E4=(BL*ER*(2.-ER))-AL*((2./3.)+RO)
      E6=(3./2.)*(SQRT(3./2.))*RH
      E13=(2.*(SQRT(3.))/3.)*((4./3.)+BL)
      E14=1.+((9./4.)*BL*(1.+ER))
      SPR=1000.
      DO 8 N=2,100
      D1=N*(N+1)
      E1=BL*ER*D1+(4./3.)+BL*(1.-ER)
      E2=(1.+BL)*D1-(2./3.)-BL
      E3=(AL*(1.+RO)+BL*(ER**2))*D1
      E5=2.*((4./3.)+BL)/D1
      PR=E6*(-((E1**2)/E2)+E3+E4+E5)
      IF(PR-SPR)4,5,5
4  SPR=PR
      N1=N
5  CONTINUE
8  CONTINUE
      PWS=(1.-(E14/SQRT(SPR)))*100.
      D2=N1*(N1+1)
      B1=BL*ER*D2+(4./3.)+BL*(1.-ER)
      B2=(1.+BL)*D2-(2./3.)-BL

```

```

B1=E1*((1.+BL)*D1+E3-(E4/D1))
B2=E1*(E12*D1+E5+(E4/D1))
B3=E1*(E13*D1+E14+(E4/D1))
C=E2*(E16*E17+(E18**2))
PR1=-C/B1
PR2=-C/B2
PR3=(-B3+SQRT((B3**2)-4.*A3*C))/(2.*A3)
IF(PR1-SPR1)4,5,5
4 SPR1=PR1
N1=N
5 CONTINUE
IF(PR2-SPR2)6,7,7
6 SPR2=PR2
N2=N
7 CONTINUE
IF(PR3-SPR3)8,9,9
8 SPR3=PR3
N3=N
9 CONTINUE
12 CONTINUE
PWS1=(1.-(E19/SQRT(SPR1)))*100.
PWS2=(1.-(E19/SQRT(SPR2)))*100.
PWS3=(1.-(E19/SQRT(SPR3)))*100.
WRITE(6,10)EH,N1,SPR1,N2,SPR2,N3,SPR3,PWS1,PWS2,PWS3
10 FORMAT(3X,F7.3,3X,3(I4,3X,E9.3,3X),3(E9.3,3X))
11 CONTINUE
END

```

BIBLIOGRAPHY

1. Becker, H. and Gerard, G., "Elastic Stability of Orthotropic Shells," *Journal of the Aerospace Sciences*, Vol. 29, No. 5, p. 505, 1962.
2. "Some Investigations of the General Instability of Stiffened Metal Cylinders," NACA-TN 905-909 and 911, 1943.
3. Klöppel, K. and Jungbluth, O., "Beitrag zum Durchschlagproblem dünnwandiger Kugelschalen," *Der Stahlbau*, 6, pp. 121-130, 1953.
4. Hayashi, T., "Torsional Buckling of Orthogonal-anisotropic Cylinders," *Corona*, Japan, 1952.
5. Van der Neut, A., "The General Instability of Stiffened Cylindrical Shells under Axial Compression," *National Luchtvaartlaboratorium*, XII, pp. 557-584, 1947.
6. Almroth, B. O. and Bushnell, D., "Computer Analysis of Various Shells of Revolution," *AIAA Journal*, Vol. 6, No. 10, pp. 1848-1855, 1967.
7. Baruch, M., "Equilibrium and Stability Equations for Stiffened Shells," *Israel Journal of Technology*, Vol. 2, No. 1, pp. 117-124, 1964.
8. Baruch, M. and Singer, J., "Effect of Eccentricity of Stiffeners on the General Instability of Stiffened Cylindrical Shells under Hydrostatic Pressure," *Journal of Mechanical Engineering Sciences*, Vol. 5, No. 1, pp. 23-27, 1963.
9. Burns, A. Bruce, "Structural Optimization of Axially Compressed Cylinders Considering Ring Stringer Eccentricity Effects," *Journal of Spacecraft and Rockets*, Vol. 3, No. 8, 1966.
10. Burns, A. Bruce, "Optimum Stiffened Cylinders for Combined Axial Compression and Internal or External Pressure," *Journal of Spacecraft and Rockets*, Vol. 5, No. 6, 1968.
11. Bushnell, David, "Symmetric and Nonsymmetric Buckling of Finitely Deformed Eccentrically Stiffened Shells of Revolution," *AIAA Journal*, Vol. 5, No. 8, 1967.
12. Bushnell, David, "Nonlinear Axisymmetric Behavior of Shells of Revolution," *AIAA Journal*, Vol. 5, No. 3, pp. 432-439, 1967.

13. Crawford, R. F. and Schwartz, D. B., "General Instability and Optimum Design of Grid-stiffened Spherical Domes," *AIAA Journal*, Vol. 3, pp. 511-515, 1965.
14. Crawford, R. F., "Effects of Asymmetric Stiffening on Buckling of Shells," *AIAA Paper 65-371*, 1965.
15. Ebner, H., "Angenaherte Bestimmung der Tragfahigkeit radial versteifter Kugelschalen unter Druckbelastung," *Proceedings I.U.T.A.M. Symposium on the Theory of Thin Elastic Shells*, North-Holland Publishing Co., Amsterdam, The Netherlands, pp. 95-121, 1960.
16. Harari, O., Singer, J., and Baruch, M., "General Instability of Cylindrical Shells with Non-uniform Stiffeners," *Israel Journal of Technology*, Vol. 5, Nos. 1 and 2, pp. 114-128, 1967.
17. Hedgepeth, John M. and Hall, David B., "Stability of Stiffened Cylinders," *AIAA Journal*, Vol. 3, No. 12, pp. 2275-2286, 1965.
18. Jones, Robert M., "Plastic Buckling of Eccentrically Stiffened Circular Cylindrical Shells," *AIAA Journal*, Vol. 5, No. 6, pp. 1147-1152, 1967.
19. Krenzke, M. A. and Kiernan, T. J., "Tests of Stiffened and Unstiffened Machined Spherical Shells under External Hydrostatic Pressure," *David Taylor Model Basin Report 1741*, 1963.
20. McElman, John A., Mikulas, Martin M., and Stein, Manuel, "Static and Dynamic Effects of Eccentric Stiffening of Plates and Cylindrical Shells," *AIAA Journal*, Vol. 4, No. 5, pp. 887-894, 1966.
21. Simitses, George J., "Buckling of Eccentrically Stiffened Cylinders under Torsion," *AIAA Journal*, Vol. 6, No. 10, pp. 1856-1860, 1967.
22. Simitses, G. J., "A Note on the General Instability of Eccentrically Stiffened Cylinders," *Journal of Spacecraft and Rockets*, Vol. 4, No. 5, pp. 473-475, 1967.
23. Singer, Joseph and Haftka, Raphael, "Buckling of Discretely Ring Stiffened Cylindrical Shells," *Israel Journal of Technology*, Vol. 6, Nos. 1 and 2, pp. 125-137, 1968.
24. Singer, J., Baruch, M., and Harari, O., "Inversion of the Eccentricity Effect in Stiffened Cylindrical Shell Buckling under External Pressure," *Journal of Mechanical Engineering Science*, Vol. 8, No. 4, 1966.

25. Stuhlman, C., Deluzio, A., and Almroth, B., "Influence of Stiffener Eccentricity and End Moment on Stability of Cylinders in Compression," *AIAA Journal*, Vol. 4, No. 5, pp. 872-877, 1966.
26. Tsao, C. H. and Ching, A., "Tests of, and Semiempirical Formulas for, Instability of Longitudinally Stiffened Shells," *Journal of Spacecraft and Rockets*, Vol. 5, No. 2, 1968.
27. Card, M. F., "Preliminary Results of Compression Tests on Cylinders with Eccentric Longitudinal Stiffeners," *NASA Langley Research Center TMX-1004*, 1964.
28. Zoelly, R., Dissertation, Zürich, 1915.
29. Schwerin, E., *Z. angew. Math. u. Mech.*, Vol. 2, p. 81, 1922.
30. Van der Neut, Dissertation, Delft, 1932.
31. von Karman, T. and Tsien, Hsue-Shen, "The Buckling of Spherical Shells by External Pressure," *Journal of the Aeronautical Sciences*, Vol. 7, No. 2, 1939.
32. Donnell, L. H., "A New Theory for the Buckling of Thin Cylinders under Axial Compression and Bending," *Trans. ASME*, Vol. 56, p. 795, 1934.
33. Donnell, L. H. and Wan, C. C., "Effect of Imperfections on Buckling of Thin Cylinders and Columns under Axial Compression," *Journal of Applied Mechanics*, Vol. 17, No. 1, p. 73, 1950.
34. Koiter, W. T., Report, Laboratory of Engineering Mechanics Dept. of Mech. Engng. Technological Univ., Delft, 1966.
35. Koiter, W. T., "Elastic Stability and Post-buckling Behavior," *Non Linear Problems*, University of Wisconsin Press, 1963.
36. Koiter, W. T., "On the Stability of Elastic Equilibrium," *NASA TT F-10*, p. 833, 1967.
37. Budiansky, Bernard and Hutchinson, John W., "A Survey of Some Buckling Problems," *AIAA Journal*, Vol. 4, No. 9, pp. 1505-1510, 1966.
38. Hutchinson, J. W., "Buckling and Initial Post-buckling Behavior of Oval Cylindrical Shells under Axial Compression," *Trans. ASME*, p. 66, 1968.
39. Koiter, W. T., "Buckling and Post-buckling Behavior of a Cylindrical Panel under Axial Compression," Report S.476, National Aeronautical Research Institute, Amsterdam, 1956.

40. Pope, G. G., "On the Axial Compression of Long Slightly Curved Panels," Aeronautical Research Council R. and M. No. 3392, London, 1965.
41. Hutchinson, J. W., "Imperfection-sensitivity of Externally Pressurized Spherical Shells," *Journal of Applied Mechanics*, Vol. 34, Series E, No. 1, pp. 49-55, 1967.
42. Thompson, J. M. T., "The Rotationally-symmetric Branching Behavior of a Complete Spherical Shell," Koninkl. Nederl. Akademie von Wetenschappen-Amsterdam reprinted from Proceedings, Series B, 67, No. 3, 1964.
43. Walker, A. C., "An Analytical Study of the Rotationally Symmetric Non-linear Buckling of a Complete Spherical Shell under External Pressure," *International Journal of Mechanical Sciences*, Vol. 10, No. 9, pp. 695-710, 1968.
44. Babcock, C. D. and Sechler, E. E., "The Effect of Initial Imperfections on the Buckling Stress of Cylindrical Shells," *Collected Papers on the Instability of Shell Structures*, NASA TN D-1510, p. 135, 1962.
45. Horton, W. H. and Durhan, S. C., "Imperfections, a Main Contributor to Scatter in Experimental Values of the Buckling Load," *International Journal of Solids and Structures*, Vol. 1, pp. 59-72, 1967.
46. Carlson, R. L., Sendelbeck, R. L., and Hoff, N. J., "An Experimental Study of the Buckling of Complete Spherical Shells," *NASA CR-550*, 1966.
47. Horton, W. H., Private Communication to L. W. Rehfield, Stanford University, 1965.
48. Hoff, N. J., "Buckling of Thin Shells," Proceedings of an Aerospace Scientific Symposium of Distinguished Lecturers in Honor of Dr. Theodore van Karman on his 80th Anniversary, May 11, 1961, The Institute of the Aerospace Sciences, New York, p. 1.
49. Rehfield, L. W., "Further Linear and Nonlinear Considerations in the Buckling and Post-buckling of Axially Compressed Circular Cylindrical Shells," Thesis, Stanford University, 1965.
50. Budiansky, B., "Buckling of Clamped Shallow Spherical Shells," *The Theory of Thin Elastic Shells*, North Holland Publishing Company, Amsterdam, 1960.
51. Stein, Manuel, "Some Recent Advances in the Investigation of Shell Buckling," *AIAA Journal*, Vol. 6, No. 12, pp. 2339-2345, 1968.

52. Horton, W. H. and Durham, S. C., "The Effect of Restricting Buckle Depth in Circular Cylindrical Shells Repeatedly Compressed to the Buckling Limit," SUDAER No. 174, Stanford University, 1963.
53. Mayers, J. and Rehfield, L. W., "Further Nonlinear Considerations in the Post-buckling of Axially-Compressed Circular Cylindrical Shells," *Proceedings of the Ninth Midwestern Mechanics Conference*, University of Wisconsin, Madison, Wisconsin, 1965.
54. Mayers, J. and Wesenberg, D. L., "The Maximum Strength of Initially Imperfect Axially-Compressed Circular Cylindrical Shells," AIAA Paper 69-91, AIAA Seventh Aerospace Sciences Meeting, New York City, New York, 1969.
55. Hutchinson, John W. and Amazigo, John C., "Imperfection-sensitivity of Eccentrically Stiffened Cylindrical Shells," *AIAA Journal*, Vol. 5, No. 3, pp. 392-401, 1967.
56. Boresi, A. P., "A Refinement of the Theory of Buckling of Rings under Uniform Pressure," *Journal of Applied Mechanics*, Vol. 22, No. 1, p. 95, 1955.
57. Armenakas, A. E. and Herrmann, G., "Buckling of Thin Shells under External Pressure," *Journal of the Engineering Mechanics Division, ASCE*, Vol. 89, No. EM3, pp. 131-146, 1963.
58. Smith, C. V. and Simites, G. J., "Effect of Shear and Load Behavior on Ring Stability," *Journal of the Engineering Mechanics Division, ASCE*, June, 1969.
59. Simites, G. J. and Cole, R. T., "Effect of Load Behavior on the Buckling of Thin Spherical Shells under Pressure," *Journal of Applied Mechanics*, June, 1968.
60. Koiter, W. T., "General Equations of Elastic Stability for Thin Shells," Seventh Anniversary Symposium on Shells to Honor Lloyd H. Donnell, April, 1966.
61. Fung, Y. C. and Sechler, E. E., "Instability of Thin Elastic Shells," *Structural Mechanics*, Proceedings of the First Symposium on Naval Structural Mechanics, Pergamon Press, London, 1960.
62. Hoff, N. J., "Thin Shells in Aerospace Structures," *Astronautics and Aeronautics*, p. 26, 1967.
63. Thompson, J. M. T., "The Elastic Instability of a Complete Spherical Shell," *The Aeronautical Quarterly*, pp. 189-201, 1962.
64. Krenzke, M. A., "Tests on Machined Deep Spherical Shells under External Hydrostatic Pressure," Report 1601 of the Structural Mechanics Laboratory of California Institute of Technology, 1962.

65. Sabir, A. B., "Large Deflection and Buckling Behavior of a Spherical Shell with Inward Point Load and Uniform External Pressure," *Journal of Mechanical Engineering Science*, Vol. 6, No. 4, p. 394, 1964.
66. Sanders, J. Lyell, Jr., "Nonlinear Theories for Thin Shells," *Quarterly of Applied Mathematics*, Vol. XXI, No. 1, pp. 21-35, 1963.
67. Sylvester, Richard J., "Membrane Volume Changes for Elliptical Domes," *Journal of the Aerospace Sciences*, Vol. 29, p. 140, 1962.
68. Lebedev, N. N., *Special Functions and Their Application*, Prentice-Hall, Inc., Englewood Cliffs, N. J., 1965.
69. Stein, Manuel, "The Phenomenon of Change in Buckle Pattern in Elastic Structures," *NASA TR R-39*, 1959.
70. Chilver, A. H., "Coupled Modes of Elastic Buckling," *J. Mech. Phys. Solids*, Vol. 15, pp. 15-28, 1967.

VITA

Robert Thurman Cole was born in Atlanta, Georgia on February 26, 1942. His parents are Joseph T. and Marjorie C. Cole. He attended the elementary and secondary schools of Marietta, Georgia, and was graduated from Marietta High School in June, 1960.

In September, 1960, Mr. Cole entered the Georgia Institute of Technology on a football scholarship, and in June, 1964, was awarded the degree of Bachelor of Science in Aerospace Engineering. He continued his education as a graduate student at the same school and received the degree of Master of Science in Aerospace Engineering in June, 1967. An NDEA Fellowship allowed him to continue under the doctoral program. Mr. Cole has been employed as an assistant scientist at the research center of Lockheed-Georgia Company in Marietta, Georgia, for several summers. He has also been employed part-time in various capacities as a graduate research assistant and a graduate teaching assistant of the Georgia Institute of Technology.

On April 22, 1969, he was married to Sara Ann Peck, daughter of Mr. and Mrs. William W. Peck of Marietta, Georgia.